

A PROPOSAL TO MEASURE  
THE DIFFRACTIVE PHOTON DISSOCIATION ON HYDROGEN

R. Cool, K. Goulianos, G. Snow, H. Sticker,  
M. Tannenbaum and S. White

The Rockefeller University  
New York, N. Y. 10021

Spokesman: K. Goulianos  
Telephone: 212/360-1761

49 pgs.

TABLE OF CONTENTS

	Page
ABSTRACT	3
I. THE PROPOSAL	4
II. THE PHYSICS	7
A. Search for new vector mesons	8
B. Measurement of the continuum	9
C. Compton Scattering	9
D. Study of the known vector mesons	10
E. Test of the Finite Mass Sum Rule	11
III. THE EXPERIMENT	13
A. TREAD - The recoil energy and angle detector	14
B. Downstream apparatus	18
C. Event rate	19
D. Mass resolution	20
E. Background	23
F. Time Schedule	24
IV. EXPERIMENTAL REQUIREMENTS	25
A. Beam and space requirements	25
B. Equipment and services	25
APPENDIX - Tests performed on a TREAD model	26
REFERENCES	28
FIGURE CAPTIONS	29

ABSTRACT

We propose to measure the diffractive dissociation of high energy photons on hydrogen,  $\gamma p \rightarrow Xp$ , in the region  $0.01 < |t| < 0.1$  (GeV/c)<sup>2</sup> and for  $M_X^2/s \lesssim 0.1$ , covering the mass range  $M_X \lesssim 5\text{GeV}$  for the presently available tagged photon energies at Fermilab (20 - 140 GeV). Specifically, we will measure the inclusive differential cross section  $d^2\sigma/dtdM_X^2$  with resolutions  $\Delta t = 0.002$  (GeV/c)<sup>2</sup> and  $\Delta M_X/M_X \lesssim 1.5\%$ .

The proposed apparatus (TREAD-The Recoil Energy and Angle Detector) consists of a 5 ft. long hydrogen gas target at 10 atm surrounded by a high pressure cylindrical drift chamber which employs four concentric circular sense wires at each endcap to measure the polar angle of the recoil proton. The chamber is generally similar in design but much simpler than the Time Projection Chamber (TPC) proposed for PEP. The pressure of the drift gas balances the target pressure and thus a mylar tube of wall thickness  $\lesssim 1$  mil may be used to contain the hydrogen. This, combined with a low density drift gas (He-7%CH<sub>4</sub>) minimizes the multiple Coulomb scattering of the recoil proton leading to a better determination of its polar angle which, in the diffractive region (low  $M_X^2/s$ ), dominates the resolution in the measurement of the mass  $M_X$ . One inch thick scintillation counters, located 10 inches away from the beam inside the high pressure vessel, measure the kinetic energy,  $T$  (hence  $|t| = 2M_p T$ ), of stopping protons. The energy loss,  $dE/dx$ , obtained by measuring the total charge collected by each sense wire, is used in combination with  $T$  to identify the recoil particle.

The experiment is particularly suited to search for new vector meson resonance structures with width in the MeV region. The sensitivity of the experiment is such that, taking into account the expected level of the continuum, a  $3.5\sigma$  effect will be seen for a resonance produced with a 10 nb cross section. In addition to the search for new and the study of the old ( $\rho^0, \omega, \phi, \psi$ ) vector mesons, we emphasize the importance of the measurement of the continuum.

We request 150 hours of testing and 1000 hours of running at a minimum tagged photon beam intensity of  $2 \times 10^6$  per pulse.

A Proposal to Measure  
The Diffractive Photon Dissociation on Hydrogen

R. Cool, K. Goulianos, G. Snow, H. Sticker  
M. Tannenbaum and S. White

The Rockefeller University  
New York, N. Y. 10021

I. THE PROPOSAL

We propose to use the Fermilab tagged photon beam to measure the diffractive dissociation of photons on hydrogen

$$\gamma + p \rightarrow X + p \quad (1)$$

in the low  $|t|$  region  $0.01 < |t| < 0.1$   $(\text{GeV}/c)^2$  and for  $M_X^2/s \leq 0.1$  covering the mass range  $M_X \leq 5$  GeV for the presently available tagged photon energies (20 - 140 GeV). Specifically, we will measure the differential cross section  $d^2\sigma/dtdM_X^2$  with resolutions  $\Delta t = 0.002$   $(\text{GeV}/c)^2$  and  $\Delta M_X \sim 30$  MeV, as well as the charge multiplicity of the dissociation products.

Considerations of event rate have limited previous photon experiments to the use of liquid hydrogen targets and thus to the range of  $|t| \geq 0.1$   $(\text{GeV}/c)^2$ . The low  $|t|$  region has been investigated only for a few exclusive reactions, e.g.,  $\rho^0 \rightarrow \pi^+\pi^-$ , with strong two-body decay channels. The apparatus we propose to build (TREAD--The Recoil Energy and Angle Detector) will employ a high pressure hydrogen gas target and thus make it possible for the first time to

study the inclusive reaction at low  $|t|$  with excellent resolution and good event rate. We are interested in Compton scattering and the known vector meson resonances, in a study of the behavior of the continuum, and in searching for new resonance structures with width in the MeV range. Such structures are expected to have very small branching ratios into  $\ell^+\ell^-$  and therefore are not easily accessible to  $e^+e^-$  colliding beams. Similarly, they could easily have been missed in hadronic production experiments because they must be searched for in exclusive channels which often have low branching ratios. In the region between the mass of the  $\phi$  and the mass of the  $J/\psi$  some broad structure is seen [ $\rho'(1250)$ ,  $\rho''(1600)$ ], and recent data from  $e^+e^-$  experiments show strong indication for resonances with widths of the order of 10 MeV. However, the data are not very precise and more work is required to understand this mass region.

TREAD is a target-detector combination similar in philosophy and performance to the apparatus we have used successfully in E-396 for the study of the diffractive dissociation of hadrons. It will consist of a 5 ft. long hydrogen gas target at 10 atmospheres, surrounded by a high pressure drift chamber, generally similar in design to the Time Projection Chamber (TPC) proposed for PEP but with a much simplified electronic detection system appropriate to our requirements. The chamber will measure accurately only the polar angle of the recoil proton. The drift gas will be pressurized to 10 atmospheres to balance the target pressure, thus enabling us to contain the hydrogen gas in a mylar tube with wall thickness  $\leq 1$  mil. The energy of the recoil protons will be measured with one inch thick scintillation counters

placed inside the high pressure gas vessel. Two scintillation counters placed immediately downstream of TREAD will determine the charge multiplicity of the dissociation products.

For hadron dissociation, the event rate in TREAD would be about 100 times greater than that of E-396. This is accomplished by having a target which is three times larger and ten times denser, and by accepting recoils over nearly 100% of the solid angle rather than 30%. This increased rate will enable us to study the diffractive photon dissociation process, which has a cross section in the order of  $10 \mu\text{b}$ , with the same statistical accuracy we have obtained in E-396 for diffractive hadron dissociation processes whose cross sections are in the  $1 \text{ mb}$  range. Specifically, we expect to obtain one clean event per  $1 \text{ nb}$  per 100 hours of running at  $10^6$  incident photons per pulse (10 sec repetition period).

We request 1000 hours of running at a minimum beam intensity of  $2 \times 10^6$  photons per pulse whose momentum is tagged to  $\pm 2\%$ . This will give us 20 events/nb or a total of about 350K diffractive events. Given the mass resolution of the experiment and the expected level of the continuum (see Section IIB), a resonance produced with  $10 \text{ nb}$  cross section will be seen as a  $3.5\sigma$  bump.

The physics goals of this experiment are almost orthogonal to those of E-516. In addition to the study of (and search for) resonance structures in the inclusive cross sections, we would like to emphasize the measurement of the continuum at these very low  $t$ -values. In the event that new structures are discovered, their decay products could eventually be studied by using TREAD to trigger the spectrometer proposed for E-516. Finally, when the Doubler becomes operative, TREAD can be used without modification to study an  $M_x^2$  region twice as large as the one proposed here.

## II. THE PHYSICS

Recent discoveries have placed the photon in a very special position among the strongly interacting particles. High energy photons are no longer viewed merely as a probe of the charge distributions of other particles, but also as a source of hadronic interactions rich in structure and surprises. Among these interactions, the diffractive dissociation of the photon,  $\gamma p \rightarrow Xp$  at low  $t$  and low  $M_x^2/s$ , is of particular interest. Through this process the photon transforms coherently (no exchange of quantum numbers) into a hadronic state while the recoiling target proton remains intact. Thus, viewed naively, diffraction dissociation provides us with a picture of the hadronic content of the photon.

It is important to emphasize the requirement of small  $M_x^2/s$  for coherence and hence the need for large  $s$  in the diffractive production of high mass states. This is evident from Fig. 1 which shows the cross section versus  $M_x^2/s$  for  $pp \rightarrow Xp$ . The enormous increase of the cross section with decreasing  $M_x^2/s$  in the region of  $M_x^2/s \lesssim 0.1$  is attributed to the coherent or diffraction dissociation process.

No measurement of the inclusive process  $\gamma p \rightarrow Xp$  exists at low  $t$  and high  $s$ . The determination of  $d^2\sigma/dtdM_x^2$  for  $\gamma p \rightarrow Xp$  requires knowledge of the incident photon momentum  $p_0$  as well as of the kinetic energy  $T$  and polar angle  $\theta$  of the recoil proton. These variables are needed to calculate  $|t| = 2M_p T$  and  $M_x^2 \approx 2p_0 \sqrt{|t|} (\cos \theta - \sqrt{|t|}/2M_p)$ . High energy tagged photon beams have become available only recently. Furthermore, owing to the small hadronic cross section of the photon, previous experiments have been restricted

to the use of liquid hydrogen targets and thus to  $|t| \gtrsim 0.1 \text{ (GeV/c)}^2$ . At small values of  $t$ , multiple scattering in the target limits the resolution in the measurement of the angle of the recoil and hence in the measurement of  $M_x$ .

For the reasons just mentioned, the study of diffractive photoproduction has been confined<sup>1</sup> to a few exclusive reactions and thus to the well known vector mesons ( $\rho^0$ ,  $\omega$ ,  $\phi$ ,  $J/\psi$ ) which have appreciable branching ratios into two- or three-body decay channels. Resonance structures with widths in the MeV range and large multiplicities in their dominant decay modes could easily have escaped detection. Recently, evidence for the existence of such resonances in the mass range from 1 to 2 GeV has been accumulating from studies of multipion production in  $e^+e^-$  colliding beam experiments<sup>2</sup>. But owing to the small production cross sections (order of 10 nb) in the exclusive channels investigated, and to the large background, the data are still sketchy.

#### A. SEARCH FOR NEW VECTOR MESONS

The experiment we propose here represents a unique tool for searching for vector meson resonances. The reasons are the following:

- 1) Diffractive production (low  $t$  and low  $M_x^2/s$ ) guarantees the identity of the quantum numbers of the hadronic state.
- 2) Inclusive production has larger cross sections. Furthermore, decay branching ratios are easily studied once a resonance is seen.
- 3) Search is performed simultaneously over the entire mass region  $M_x^2/s \lesssim 0.1$ . At the same time, the  $s$  and  $t$  dependence are measured. Relative production cross sections are easily determined.

- 4) The "background" under the resonances is expected to be smooth and have the characteristic  $1/M_x^2$  shape that is observed in diffractive hadron dissociation. Thus, resonance peaks are easily identified and extracted.

## B. MEASUREMENT OF THE CONTINUUM

If the hadronic constituent of the photon behaves like an ordinary hadron, the differential cross section  $d^2\sigma/dtdM_x^2$  is expected to display the following characteristics<sup>3</sup>:

- 1) Exponential  $t$  behavior in the region  $|t| \lesssim 0.1$  (GeV/c)<sup>2</sup>.
- 2)  $1/M_x^2$  dependence in the region  $M_x^2/s \lesssim 0.1$ .
- 3) Factorization of the diffractive vertex. It is a consequence of this rule that the diffractive cross section  $hp \rightarrow Xp$  scales as the total cross section  $hp \rightarrow \text{anything}$ . From known data<sup>4</sup> on  $pp \rightarrow Xp$  one obtains the estimate

$$\frac{d^2\sigma}{dtdM_x^2} (\gamma p \rightarrow Xp) = \frac{\sigma_T^{\gamma p}}{\sigma_T^{pp}} \frac{d^2\sigma}{dtdM_x^2} (pp \rightarrow Xp) \approx \frac{20}{M_x^2} e^{7t} \mu b \cdot \text{GeV}^{-4} \quad (2)$$

It is, perhaps, worth pointing out that the  $t$  dependence may turn out to be different from the above since the notion of factorization is strictly a  $t = 0$  phenomenon. Of course, if the photon is not like an ordinary hadron, none of the above features need be true.

## C. COMPTON SCATTERING

An experiment currently in progress at Fermilab (E-152) is measuring this process for  $|t| \gtrsim 0.1$  (GeV/c)<sup>2</sup>. Extrapolation of  $d\sigma/dt$  to  $t = 0$  should be

consistent (via the optical theorem) with the total cross section measurements. However, no reliable extrapolation can be performed in the absence of data at small  $t$ . Our experiment will measure  $d\sigma/dt$  in the region  $0.01 < |t| < 0.1$   $(\text{GeV}/c)^2$  and thus complement the results of E-152.

#### D. STUDY OF THE KNOWN VECTOR MESONS

Photoproduction of  $\rho^0$ ,  $\omega$ , and  $\phi$  has been studied extensively only in the energy region  $\lesssim 10$  GeV. The  $\rho^0$  data are very extensive, but owing to the poor understanding of the dipion continuum, the extrapolated forward cross section as well as the width of the  $\rho^0$  cannot be determined accurately from photoproduction experiments. The understanding of the  $\omega$  is complicated by the non-diffractive one-pion exchange contribution, which is important at low energies, and discrepancies as large as 20% exist among the various experiments in the extrapolated forward diffractive cross sections. Finally, the magnitude of the  $\phi$  photoproduction cross section is about one half of that predicted by a quark-model analysis<sup>1</sup>.

Our experiment will measure the  $s$  and  $t$  dependence of the diffractive photoproduction of  $\rho^0$ ,  $\omega$ , and  $\phi$  in the region of  $0.01 < |t| < 0.1$   $(\text{GeV}/c)^2$  and at energies higher than 10 GeV. At these energies, the non-diffractive contributions and the real parts of the forward production amplitudes are expected to be small. This will simplify the interpretation of the data and, combined with the measurement of the continuum, will undoubtedly lead to a better understanding of the hadronic structure of the photon. The simultaneous study of all three mesons in the same (inclusive) process may also help to resolve some of the problems mentioned above.

Of course, the  $J/\psi$  as well as possible new vector mesons will also be studied simultaneously with the  $\rho^0$ ,  $\omega$ , and  $\phi$ .

### E. TEST OF THE FINITE MASS SUM RULE

The FMSR is an extension of the finite energy sum rule for total cross sections<sup>5</sup>. It derives from the hypothesis that the diffractive cross sections can be described either by s-channel resonance or by t-channel Reggeon exchanges. Schematically,

$$\sum_R \text{Diagram 1} = \sum_i \text{Diagram 2} \quad (3)$$

It has been found experimentally<sup>6,7</sup> that the low  $t$  diffractive cross sections of hadrons satisfy the first-moment FMSR. This states that the value of the function

$$f(s, \nu, t) = \nu \frac{d^2\sigma}{dt d\nu} \quad (4)$$

where  $\nu = M_X^2 - M_h^2 - t$  (the cross-symmetric variable), averaged over a large enough interval in  $\nu$  to include local resonances, is independent of  $\nu$ . A test of this rule<sup>6</sup> for  $pd \rightarrow Xd$  is displayed in Fig. 2. The rule holds to within the experimental accuracy of a few per cent. Tests performed on the dissociation of pions and kaons on hydrogen<sup>7</sup> also support the validity of this rule. In all cases, the low mass enhancements have just the right magnitude and  $t$  dependence to satisfy the first-moment FMSR at small values of  $t$ .

Regardless of the nature of the hadronic constituent of the photon, diffractive photon dissociation should also satisfy the first-moment FMSR. However, the magnitude and shape of the continuum will depend on the photon's hadronic structure. For example, in vector dominance models one does not expect any diffractive component in the mass region below the  $\rho^0$ . Through the FMSR, the presence of such a component will also be reflected in the magnitude and  $t$  dependence of the high mass continuum.

### III. THE EXPERIMENT

The measurement of the inclusive cross section  $d^2\sigma/dtdM_x^2$  for  $\gamma p \rightarrow Xp$  in the region  $0.01 < |t| < 0.1$  (GeV/c)<sup>2</sup> and  $M_x^2/s \lesssim 0.1$  requires a tagged photon beam, a hydrogen target and a detector that measures the energy and polar angle of recoil protons in the region  $5 < T < 50$  MeV and  $45^\circ < \theta < 90^\circ$ . The variables  $t$  and  $M_x^2$  are then determined from the measured quantities  $p_0$ ,  $T$ , and  $\theta$  as follows:

$$\begin{aligned} t &= -2M_p T \\ M_x^2 &\approx 2p_0 \sqrt{|t|} (\cos \theta - \sqrt{|t|}/2M_p) \end{aligned} \quad (5)$$

A schematic drawing of the experimental arrangement is shown in Fig. 3. Downstream apparatus is used to look at the dissociation products.

Fig. 4 shows the mass spectrum expected from 50 GeV photons. Typical mass resolutions are presented in Fig. 5. Thus, a resolution of  $\Delta M_x \approx \pm 30$  MeV may be obtained at this energy with  $\Delta p_0/p_0 = \pm 0.02$ ,  $\Delta t = \pm 0.002$  (GeV/c)<sup>2</sup> and  $\Delta\theta = \pm 3$  mrad. The required resolution in  $t$  is achieved by stopping the protons in scintillation counters and using the pulse height to measure their energy. The resolution in  $\theta$  is limited by the multiple Coulomb scattering in the target-detector combination. A liquid hydrogen target is inadequate. For example, the multiple scattering of 25 MeV protons ( $|t| = 0.05$ ) in 1 cm of liquid hydrogen results in  $\Delta\theta = \pm 10$  mrad. The energy loss in the target degrades the resolution even further. Good angular resolution for low energy recoils requires the use of a gas target with thin walls. The multiple scattering due to the material along the path of the protons inside the recoil detector

must also be kept small. Event-rate considerations necessitate the use of a high pressure target and detection of recoils over a large solid angle. Finally, the detector must be capable of handling the practically infinite sea of low energy recoil electrons from the interactions of the beam in the target. A target-detector combination with these properties is described below. Tests performed on a one-half size model are discussed in the Appendix.

#### A. TREAD - THE RECOIL ENERGY & ANGLE DETECTOR

The detector we propose to build incorporates a hydrogen gas target at 10 atm and a recoil spectrometer. A schematic drawing is shown in Fig. 6. The target is three inches in diameter and five feet long. It is surrounded by a drift chamber which is also pressurized to 10 atm to balance the target pressure and thus enable us to contain the hydrogen in a mylar tube with wall thickness  $\leq 1$  mil.

The drift chamber is similar in principle to the Time Projection Chamber (TPC) proposed for PEP. However, since the energy loss ( $dE/dx$ ) of the recoil particles need not be known accurately, only four sense wires are employed on each endcap. Delay lines are used to measure the azimuthal angle. This information is useful for rejecting events which do not originate in the interaction region. The total charge collected by each sense wire is also recorded. With four wires, we expect a 10% accuracy in the measurement of  $dE/dx$ . Combined with the measurement of the total energy  $E$ , this information is used to identify the recoil particle. An alternate way of accomplishing this is by measuring the time-of-flight (TOF) of the recoil. This method was used successfully in

E-396 and will also be used in this experiment as a check on the  $dE/dx$  measurement and for background rejection. The energy of the recoil particle is measured by one inch thick scintillation counters placed 10 inches away from the axis inside the high pressure gas vessel. Particles penetrating these counters register on anti-counters placed immediately behind. The pulse-height counters cover about 80% of the azimuthal angle.

The drift field will be 120 kV over the 30-inch maximum drift distance. The drift velocity in a given gas mixture depends on the value of  $E/p$  where  $E$  is the electric field and  $p$  the pressure of the gas. In our case,  $E/p \approx 0.2$  (V/cm)/torr. A low-density drift gas will be used in order to minimize multiple scattering. Helium with 7% methane works well. The multiple scattering of 25 MeV protons ( $|t| = 0.05$ ) in traversing the target (1.5 inches), the mylar wall (0.5 mil) and four inches of drift gas distributed over the measured track results in  $\Delta\theta = \pm 4$  mrad. Combined with a drift chamber resolution of 0.3 mm, the overall angular resolution will be  $\pm 5$  mrad. This is a conservative estimate. For  $p_0 = 50$  GeV/c,  $\Delta p_0/p_0 = 0.02$  and  $\Delta t = \pm 0.002$  (GeV/c)<sup>2</sup> the mass resolution around  $M_x = 1.5$  GeV is then  $\Delta M_x = \pm 39$  MeV. In Fig. 5,  $\Delta\theta = \pm 3$  mrad was used. This can be realized with hydrogen as a drift gas and with 0.15 mm spatial resolution. We are presently investigating the possibility of using hydrogen in the drift chambers.

The drift velocity,  $V_d$ , in He-CH<sub>4</sub> mixtures is a function of the CH<sub>4</sub> concentration and of  $E/p$ . Results of measurements we have performed on such mixtures show that, for 7% CH<sub>4</sub> in He, the drift velocity in the region  $0.05 < E/p < 0.25$  (V/cm)/torr is approximately given by

$$V_d \approx 22 (E/p)^{0.7} \text{ mm}/\mu\text{sec} \quad (6)$$

Thus, the maximum drift time for the 30 inch path at  $E/p = 0.2$  will be about 100  $\mu$ sec.

Because of the dependence of the drift velocity on  $E/p$ , the electric field and the pressure (hence the temperature) of the drift gas must be kept constant over the drift volume and as a function of time. Spatial  $E/p$  variations will affect the resolution in the measurement of the polar angle of the recoil. Variations in time change the overall drift velocity and thus also affect the measurement of the angle. Since the angle is measured by the difference in the time of arrival of drifting electrons on adjacent sense wires, the effect increases as the polar angle decreases. For  $\theta = 45^\circ$ , the change in the angle due to a variation in  $E/p$  is given by (see Eq. 6)

$$\Delta\theta = 0.7 \left[ \frac{\Delta(E/p)}{(E/p)} \right].$$

Thus, in order to achieve  $\Delta\theta = \pm 3$  mrad,  $E/p$  must be kept constant to within  $\pm 0.4\%$ . Temporal variations can be taken care of by constantly calibrating the overall drift velocity. For this purpose, electrons from a beta source traversing the chamber perpendicular to the axis and triggering a small counter may be used. Spatial variations are avoided by carefully shaping the electric field. This is achieved with a series of coaxial metal rings whose potential is set to the proper value by a bleeder resistor chain drawing current supplied by the HV plate. We have calculated that forty such rings equally spaced along the 30 inch drift distance should be adequate. In order to avoid corona discharges, the rings will be made of wire 1/8 inch in diameter. Obviously, such massive rings should not be located in the path of the recoil protons and therefore will be placed on the outside of the scintillation counters. A 3/8 inch thick lucite tube will serve to insulate the HV plate and the field shaping rings from the high pressure steel vessel.

A 1 kGauss axial magnetic field will be set up inside the drift volume. This will prevent low energy Compton electrons from reaching the pulse-height counters and causing unwanted triggers. The kinematics allows only recoil electrons with energy less than 1 MeV to have polar angles greater than  $45^\circ$ . In the absence of the magnetic field, these electrons would be free to trigger the apparatus. The 1 kGauss field is adequate to confine them within the three inch diameter mylar tube of the hydrogen target. Proton recoils of interest have momentum greater than 100 MeV/c and will not be affected appreciably by the magnetic field.

The magnet will consist of two coils wound in separate layers around the two-foot diameter steel pipe that houses the recoil spectrometer. Each coil will be made of a single piece of copper pipe 700' long by 5/8" OD by 0.049" wall thickness, and will be wound in 100 turns along the six foot length of TREAD. Vinyl tubing will be used for electrical insulation. To set up the desired field, 750A (at 48V) will be supplied to each coil. The total power dissipation of the magnet will be 73 kWatts and water-flow will be required for cooling. With 50 psi of water pressure at the input, the flow through each coil will be  $2.8 \text{ ft}^3/\text{min}$  and the temperature rise of the water will be  $6.5^\circ\text{C}$ . To avoid building of temperature gradients along the length of the spectrometer, the water in the two coils will be flowed in opposite directions. The magnetic flux will be absorbed by the iron endcaps and will be returned by a 30 inch dia. by 1/2 inch thick iron pipe surrounding the spectrometer. Cross sections of the entire apparatus are shown on Figures 7 and 8.

The trigger will consist of a count in the pulse-height counters in coincidence with a pulse from the counter array of the tagging system and in anti-coincidence with the anti-counters, indicating a stopping recoil. A track of

angle between  $45^\circ$  and  $90^\circ$  with respect to the axis of the spectrometer will be required in the trigger by forming a 15  $\mu\text{sec}$  wide coincidence of the four sense wires with a 100  $\mu\text{sec}$  gate generated by the counters. In order to correlate the count in a PH counter with a track, and thus avoid triggering on background, information on the azimuthal angle of the track must be incorporated in the trigger. This will be accomplished by segmenting each sense wire into two semicircles, rotating the segments of a wire by  $45^\circ$  relative to the segments of the smaller diameter neighboring wire, and placing each pair of the 16 pulse-height counters in coincidence with the appropriate four segments (see Fig. 9). With this arrangement, TREAD is practically divided into eight independent spectrometers, with each spectrometer covering  $45^\circ$  of the azimuthal angle.

#### B. DOWNSTREAM APPARATUS

Simple apparatus will be used downstream of TREAD to measure the charge multiplicity  $N_c$  and the total neutral energy of the photon dissociation products.

The multiplicity will be determined by measuring the pulse height in two 1/4 inch thick scintillation counters placed immediately after the recoil spectrometer. Such an arrangement was used successfully in E-396. Fig. 10 shows the charge multiplicity distribution of diffractive masses in the region  $1 < M_x < 2$  GeV obtained in E-396 from  $\pi^-p \rightarrow Xp$  at 100 GeV/c. The resolution in the measurement of  $N_c$  is approximately  $\pm 10\%$ .

The neutral energy will be measured by a crude lead-glass array located about ten feet downstream. A hole in the middle of the array will permit the photon beam to pass through undisturbed.

The combination of multiplicity and neutral energy cuts introduced in the data is a powerful tool for separating close-lying resonances which have different decay modes. This is demonstrated in Figures 11 and 12 with data from E-396 for  $\pi^-p \rightarrow Xp$  at 100 GeV/c. In Fig. 11, one sees that the requirement of  $N_c = 1$  and no neutral energy eliminates the diffraction dissociation component and leaves a clean elastic peak. Fig. 12 shows the effect of requiring  $N_c = 3$ . The elastic peak is reduced dramatically allowing the  $A_1$  enhancement to stand out and make the  $A_3$  visible. This technique, applied to photoproduction, could be particularly useful in separating the  $\omega$  from the  $\rho^0$ .

We have described here what would be our minimum requirement of a downstream detector. Of course, if the spectrometer facility presently under construction for use in E-516 were to be triggered by TREAD, it would provide us with a much more detailed analysis of the diffractive states.

### C. EVENT RATE

Assuming a beam intensity of  $2 \times 10^6$  tagged photons per pulse, a 10 sec repetition period, a 1.5m long hydrogen gas target at 10 atm ( $\rho = 0.9 \times 10^{-3} \text{g/cm}^3$ ), an 80% acceptance of recoils over the azimuthal angle, and an exponential distribution in  $t$  with a slope  $b = 7 \text{ (GeV/c)}^{-2}$ , the number of events within the region  $0.01 < |t| < 0.1 \text{ (GeV/c)}^2$  will be:

$$\begin{aligned}
 N &= (2 \times 10^6/\text{pulse}) \times (0.1 \text{ pulses/sec}) \times (3.6 \times 10^6 \text{ sec/1000 hours}) \\
 &\times (0.9 \times 10^{-3} \text{ g/cm}^3) \times (6 \times 10^{23} \text{ protons/g}) \times (1.5 \times 10^2 \text{ cm}) \\
 &\times (10^{-33} \text{ cm}^2/\text{nb}) \times (0.8 \text{ geometric acceptance}) \\
 &\times (0.435 \text{ t-acceptance}) \\
 &= 20 \text{ events/nb for 1000 hours of running at } 2 \times 10^6 \text{ photons per pulse}
 \end{aligned}$$

The number of events expected for various diffractive photon dissociation processes is listed in the Table below:

TABLE OF EVENT RATES  
( $\gamma p \rightarrow Xp$ )

PARTICLE <u>X</u>	CROSS SECTION <u><math>\sigma</math> (<math>\mu\text{b}</math>)</u>	NUMBER OF EVENTS <u>(1000 hrs, <math>2 \times 10^6</math>/pulse)</u>
$\gamma$	0.1	2,000
$\rho^0$	10.0	200,000
$\omega$	1.4	28,000
$\phi$	0.45	9,000
new particle	0.010 (assumed)	200
continuum	5.4	108,000

The cross section for the continuum was obtained from Eq. (2), section IIB. A total of 350,000 events will be obtained in 1,000 hours of running. This amounts to one event per pulse, a rate comparable to that of E-396.

#### D. MASS RESOLUTION

The resolution in the measurement of  $M_X$  is obtained by differentiating the mass formula,  $M_X^2 \approx 2p_0 \sqrt{|t|} (\cos \theta - \sqrt{|t|}/2M_p)$ . It is instructive to express the fractional resolution in  $M_X^2$  as a function of the variable  $a \equiv M_X^2/s$  which is a measure of the diffractive character of the dissociation process as explained in Section II and demonstrated by Fig. 1. The individual contributions of the errors in  $p_0$ ,  $t$  and  $\theta$  to  $\Delta M_X^2/M_X^2$  are:

$$\left( \frac{\Delta M_x^2}{M_x^2} \right)_{p_0} = \frac{\Delta p_0}{p_0} \quad (7)$$

$$\left( \frac{\Delta M_x^2}{M_x^2} \right)_t = \frac{1}{2} \left| \frac{\Delta t}{t} - \frac{1}{2} \frac{\Delta t}{a M_p^2} \right| \quad (8)$$

$$\left( \frac{\Delta M_x^2}{M_x^2} \right)_\theta = \frac{\sqrt{|t|}}{a M_p} \left[ 1 - \left( \frac{a M_p}{\sqrt{|t|}} + \frac{\sqrt{|t|}}{2 M_p} \right)^2 \right]^2 \Delta\theta \approx \frac{\sqrt{|t|}}{a M_p} \Delta\theta \quad (9)$$

In Fig. 13 we plot  $\Delta M_x^2/M_x^2$  versus  $a$  for  $|t| = 0.05 \text{ (GeV/c)}^2$  using  $\Delta p_0/p_0 = 0.02$ ,  $\Delta t = 0.002 \text{ (GeV/c)}^2$  and  $\Delta\theta = 5 \text{ mrad}$ . In the region  $0.05 < M_x^2/s < 0.1$ ,  $\Delta M_x^2/M_x^2$  is approximately constant:

$$\left( \frac{\Delta M_x^2}{M_x^2} \right)_{|t| = 0.05} \approx 0.03 \quad (10)$$

$(0.05 < M_x^2/s < 0.1)$

Since  $\Delta M_x^2 \approx 2M_x \Delta M_x$ , the expected fractional mass resolution is

$$\frac{\Delta M_x}{M_x} \approx \pm 1.5\% \quad (11)$$

In the beam momentum interval  $20 < p_0 < 100 \text{ GeV/c}$ , the above region of  $M_x^2/s$  covers the mass range  $1.4 < M_x < 4.3 \text{ GeV}$ .

As  $M_x^2/s$  decreases deeper into the diffractive region, the mass resolution becomes worse. This is due to the uncertainty in the angle  $\theta$ . Thus, good angular resolution is crucial to the study of truly diffractive photon dissociation.

The error in the measurement of the angle is dominated by the multiple Coulomb scattering of the recoil protons. The uncertainty in the projected scattering angle is

$$\Delta\theta_{\text{proj}} = \frac{0.014}{|t|} \sqrt{\frac{L_1}{L_{1,\text{rad}}} + \frac{L_2}{L_{2,\text{rad}}} + \frac{1}{3} \frac{L_3}{L_{3,\text{rad}}}} \quad (12)$$

where the subscripts 1, 2 and 3 stand for the hydrogen target, the mylar wall and the drift gas distributed over the measured track (factor of 1/3).

The values of  $L_i$  and  $L_{i,\text{rad}}$  are listed below:

<u>Index</u> $i$	<u>Material</u>	<u><math>L_i</math> (cm)</u>	<u><math>L_{\text{rad}}</math> (cm)</u>
1	H <sub>2</sub> at 10 atm (target)	3.8	$7 \times 10^4$
2	Mylar (target wall)	0.0013	28.7
3	He-7% CH <sub>4</sub> at 10 atm (drift gas)	10.0	$3.5 \times 10^4$

With these values and for  $|t| = 0.05 \text{ (GeV/c)}^2$ , Eq. (12) yields  $\Delta\theta_{\text{proj}} = 3.9 \text{ mrad}$ . To obtain the total error in  $\theta$  one must add in quadrature the uncertainty arising from the measurement of the drift time. A conservative estimate of 0.3mm accuracy in the position measurement by each of four sense wires equally spaced over 10cm gives  $\Delta\theta_{\text{drift}} = \pm 3 \text{ mrad}$ . Thus, the overall uncertainty in the angle is expected to be  $\leq 5 \text{ mrad}$ .

An estimate of the level of the cross section to which this experiment is sensitive to "seeing" a narrow resonance (width smaller than the mass resolution) requires knowledge of the cross section due to the continuum contained within the resolution width,  $\pm \Delta M_X^2$ . This can be obtained from Eqs. (2) and (10),

$$\sigma (\text{within } \pm \Delta M_X^2) \approx 170 \text{ nb} \quad (13)$$

Hence, under a resonance bump of  $N$  events produced with a cross section of  $\sigma_R$  nanobarns, there are  $N \times 170/\sigma_R$  events due to the continuum. The statistical significance of the bump in standard deviations is  $n_{s.d.} = N/\sqrt{N \times 170/\sigma_R}$ . For a run of  $C$  events per nanobarn,  $N = C\sigma_R$  and therefore

$$n_{s.d.} = \sigma_R (\text{nb}) \sqrt{\frac{C(\text{Events/nb})}{170 \text{ nb}}} \quad (14)$$

Thus, with 20 events/nb expected in 1,000 hours of running, the statistical significance of a bump produced with a cross section  $\sigma_R = 10 \text{ nb}$  will be 3.5 standard deviations.

#### E. BACKGROUND

Electrons from  $\gamma + e \rightarrow \gamma + e$  (Compton scattering) recoiling at angles greater than  $45^\circ$  have energies less than 1 MeV and will be confined by the magnetic field within the walls of the target. Electron-positron pairs are produced at very forward angles (order of  $m_e/E_\gamma$ ) and thus, again, remain within the target walls.

Spurious tracks from charged particles incident at large angles within the 100  $\mu\text{sec}$  drift time of an event could cause problems if the rate of

such tracks were high enough. Since TREAD is divided into eight independent sectors, and since the electronics and the analysis can handle at least one extra track per event, the rate of spurious tracks would have to be greater than  $10^5$ /sec for the problem to become serious. We do not anticipate such a high rate of extra tracks.

#### F. TIME SCHEDULE

We estimate that TREAD can be ready for installation by the end of 1979.

#### IV. EXPERIMENTAL REQUIREMENTS

##### A. BEAM AND SPACE REQUIREMENTS

The experiment requires a tagged photon beam of intensity  $\geq 2 \times 10^6$  per pulse and  $\Delta p/p \lesssim 0.02$ . We understand that a beam of  $6 \times 10^6$  tagged photons per pulse with  $\Delta p/p = 0.05$  is planned for use by E-516. We do not anticipate any problems in decreasing the momentum bite of the tagging system at the expense of intensity.

TREAD is a small, portable apparatus. It could easily be rolled in and out of the beam if this would facilitate the scheduling of experiments. Fig. 3 shows the experimental arrangement. TREAD occupies approximately a 10 ft. section along the beam line. The downstream lead-glass array is also small and portable.

##### B. EQUIPMENT AND SERVICES

No special equipment or services are requested from Fermilab other than power and water supply for our magnet as well as what is necessary to operate the tagged photon beam. However, we do request the use of a PDP 11/45 computer and of standard PREP electronics.

All data analysis will be performed on Rockefeller University computers.

APPENDIX

Tests Performed on a TREAD Model

We have built a one-half size model of TREAD and we are presently testing it with cosmic rays. Fig. 14 is a photograph of the model showing (on the left) the endcap assembly and (on the right) the high pressure vessel. A more detailed photograph of the endcap assembly is shown on Fig. 15. The field shaping rings, made of 1/16" dia. copper tubing and spaced 3/8" apart, are clearly visible. The model is identical in design to TREAD, except that it employs only two scintillation counters (see Fig. 15) and uses a different sense wire arrangement, appropriate to cosmic ray testing (see Fig. 16). The counters are 1/2" x 1 1/2" x 15", equal in length to the maximum drift distance.

A computer is used on-line to take cosmic ray data for all tracks that trigger the counters. Thus, data are accumulated simultaneously for tracks of various angles distributed over the entire drift space. In addition to the drift time of each wire, the pulse height of the wires is recorded.

Results from a run in which standard DWC electronics were used are presented in Figures 17-19. The parameters of the run were:

Drift gas	He - CH <sub>4</sub> (10% by volume)
Pressure	p = 5 atm = 5 x 760 torr
High Voltage	-HV = 25 kV
Max. Drift Distance	38 cm (15 inches)
E/p - (Volt/cm)/torr	E/p = 0.17

Fig. 17 shows the pulse height obtained from a sense wire as a function of drift time,  $t_D$ . The pulse height is constant, independent of  $t_D$ . No attenuation

is observed even for the largest drift time. The maximum drift time, corresponding to  $x_{D,max}$ , is 54.5  $\mu$ sec. Hence,

$$\text{Drift velocity } V_D = 7.0 \text{ mm}/\mu\text{sec}$$

The pulse height distribution, integrated over the entire drift distance, is shown in Fig. 18. The width of the distribution is approximately  $\pm 20\%$ . Thus, with four sense wires, the energy loss ( $dE/dx$ ) could be measured to  $\pm 10\%$ , which is adequate for our requirements.

The resolution in the position measurement is obtained by fitting a line to the drift times measured by four of the sense wires and plotting the difference of the time measured by the fifth wire from the time predicted by the fit,  $\Delta t_D = t_D - t_{D, \text{fit}}$ . Such a plot is shown as a function of  $t_D$  in Fig. 19. The systematic shift in  $\Delta t_D$  is caused by the inhomogeneity of the electric field near the sense wire plate. This is well understood and can be corrected. The width of  $\Delta t_D$  increases with  $t_D$ . Translating into distance, one finds that

$$\sigma_x \approx 100\mu \sqrt{x(\text{cm})}$$

This is consistent with the width expected from the diffusion of an electron bunch as it drifts over a distance  $x$ . Since the diffusion width is  $\sim \sqrt{x/p}$ , the resolution at 10 atm will be  $\sigma_x(10 \text{ atm}) = 70\mu \sqrt{x(\text{cm})}$ . This would result in  $\Delta x_{max} = \pm 610\mu$  at  $x_{max} = 76 \text{ cm}$ , the maximum drift distance in TREAD. However, a substantial improvement in the resolution is expected by the use of electronics capable of locating the center of the arriving electron bunch. We are presently experimenting with zero-crossing discriminators.

REFERENCES

1. T.H. Bauer et al., Reviews of Modern Physics 50, 261 (1978).
2. See, for example, Rapporteur's report presented by G.J. Feldman (SLAC) at the XIX International Conference on High Energy Physics, Tokyo, Japan (1978).
3. K. Goulianos, "Diffractive Hadron Dissociation," Rockefeller University Report No. C00-2232A-59 (Paper presented to the XIII<sup>th</sup> Rencontre de Moriond Conference, France (March 1978)).
4. Y. Akimov et al., Phys. Rev. Letters 39, 1432 (1977).
5. S.D. Ellis and A.I. Sanda, Phys. Letters 41B, 87 (1972).
6. Y. Akimov et al., Phys. Rev. D14, 3148 (1976).
7. Fermilab Experiment E-396 on Hadron Diffraction Dissociation (Analysis currently in progress) - Cool, Goulianos, Segler, Sticker and White.

FIGURES

- Fig. 1 - The invariant differential cross section  $d^2\sigma/dtd(M_X^2/s)$  for  $pp \rightarrow Xp$  at  $t = -0.042 \text{ (GeV/c)}^2$  and  $s$  from 13 to  $500 \text{ GeV}^2$ .
- Fig. 2 - Test of the first-moment Finite Mass Sum Rule for  $pd \rightarrow Xd$ .
- Fig. 3 - Experimental arrangement.
- Fig. 4 - Mass spectrum expected from 50 GeV photons.
- Fig. 5 - Expected mass resolutions at 50 GeV/c.
- Fig. 6 - TREAD - Schematic drawing.
- Fig. 7 - TREAD - Side view.
- Fig. 8 - TREAD - Front view.
- Fig. 9 - TREAD - Arrangement of sense wires.
- Fig. 10 - Pulse height distribution of "multiplicity" counters of E-396 for  $\pi^-p \rightarrow Xp$  at 100 GeV/c and  $1 < M_X < 2 \text{ GeV}$ .
- Fig. 11 - Number of events versus  $M_X^2$  for  $\pi^-p \rightarrow Xp$  at 100 GeV/c (from E-396). The requirement of charge multiplicity one and no neutral energy eliminates all events but the elastic.
- Fig. 12 - Number of events with charge multiplicity 3 versus  $M_X^2$  for  $\pi^-p \rightarrow Xp$  at 100 GeV/c (from E-396). The requirement of  $N_C = 3$  practically eliminates the elastic peak and makes the  $A_3$  peak visible.
- Fig. 13 - Fractional resolution  $\Delta M_X^2/M_X^2$  vs  $M_X^2/s$ .
- Fig. 14 - TREAD Model (photo): Endcap assembly (left) and high pressure vessel (right).
- Fig. 15 - TREAD Model (photo): Endcap assembly.

Fig. 16 - TREAD Model: Scintillation counter and sense wire arrangement.

Fig. 17 - TREAD Model: Pulse height versus drift time.

Fig. 18 - TREAD Model: Pulse height distribution of a sense wire (integrated over a drift distance of 38 cm).

Fig. 19 - TREAD Model: Drift time deviation of a sense wire from the fit,

$$\Delta t_D = t_D - t_{D, \text{fit}}$$

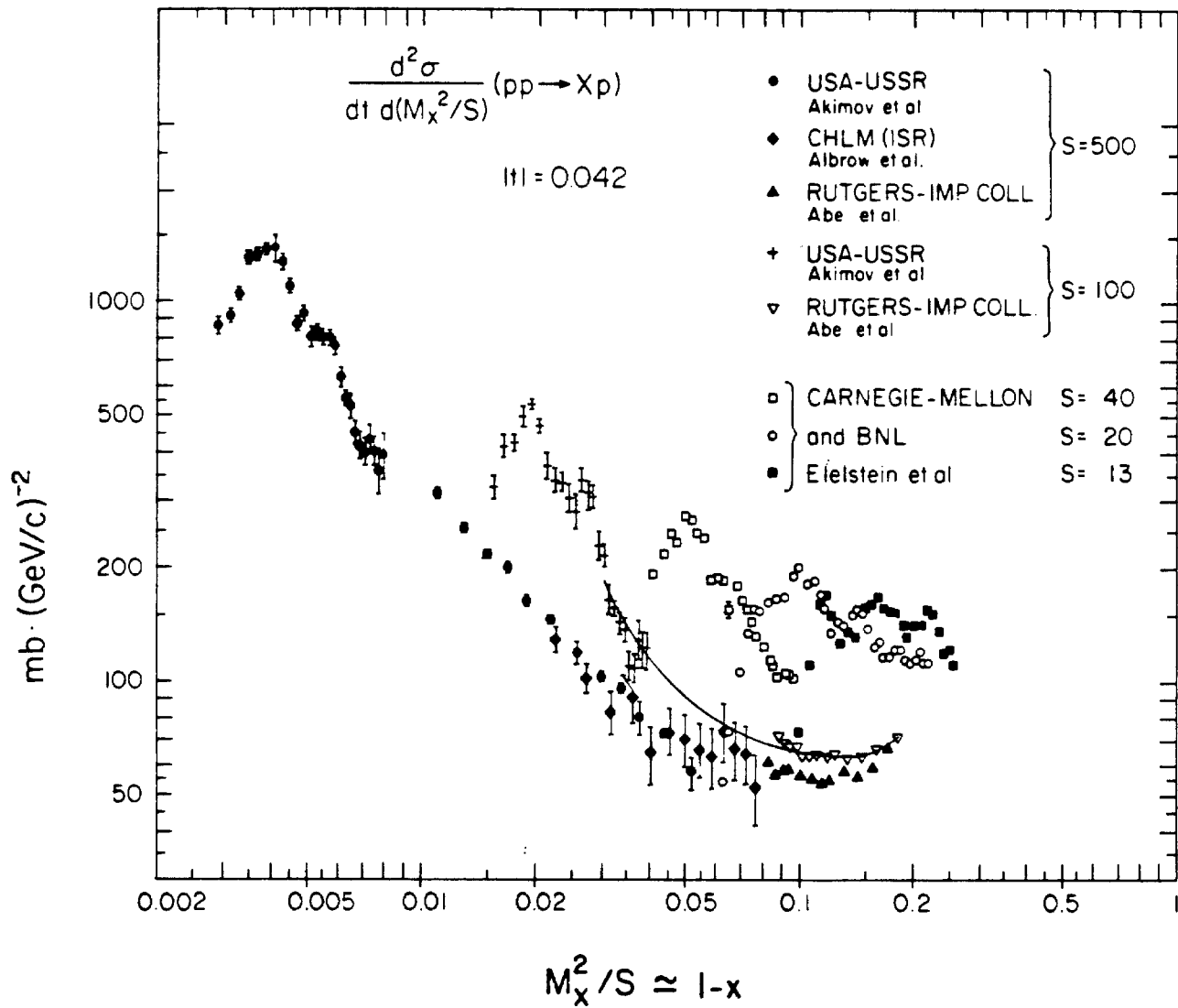


FIG. 1

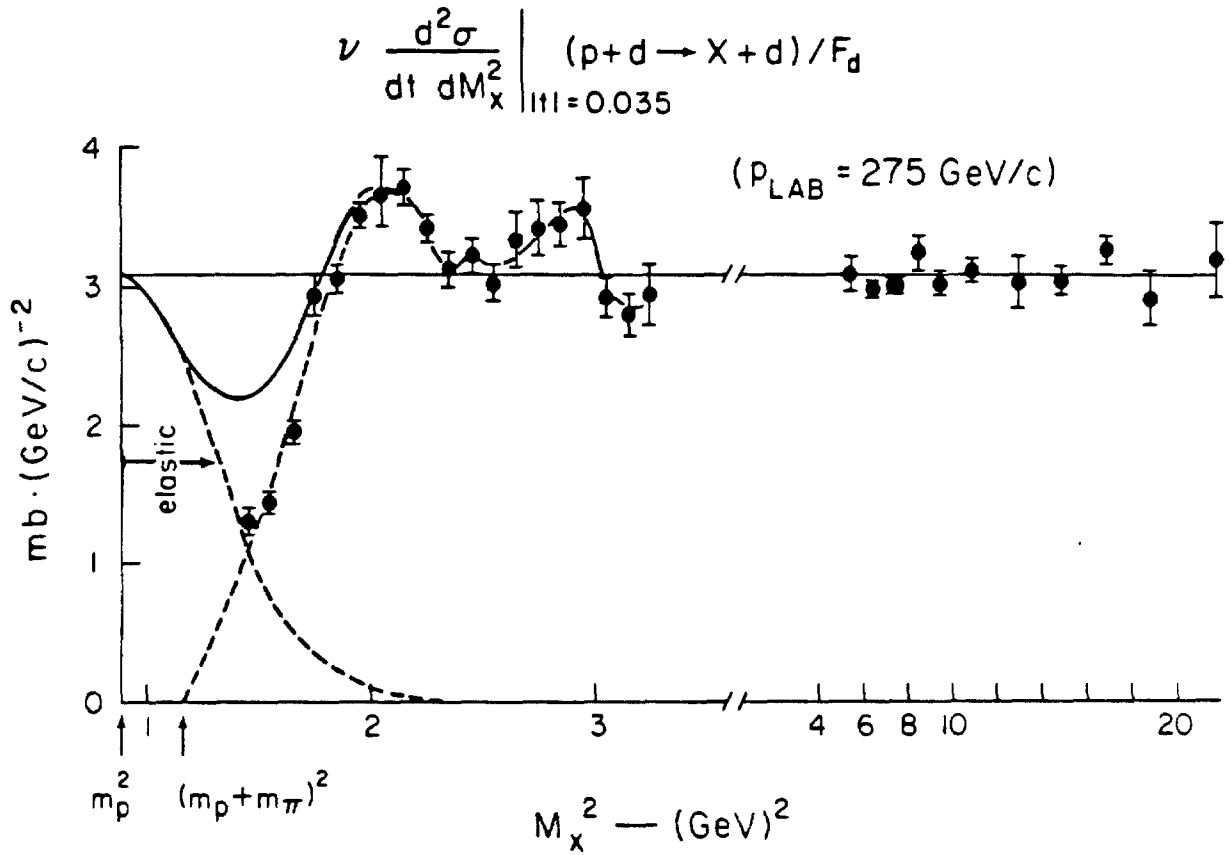


FIG. 2 - Test of the first-moment Finite Mass Sum Rule for  $pd \rightarrow Xd$ :  
 Values of  $\nu(d^2\sigma/dtdM_x^2)$  vs  $M_x^2$  for  $p_{\text{lab}} = 275 \text{ GeV}/c$  and  
 $|t| = 0.035 \text{ (GeV}/c)^2$ . Since  $t$  is fixed,  $d\nu = d(M_x^2 - M_p^2 - t)$   
 $= dM_x^2$ . The area named "elastic" is equal to the value of  
 $|t| d\sigma^{el}/dt$  and has been given a  $1/2$  Gaussian shape for  
 pictorial purposes. The sum

$$|t| \frac{d\sigma^{el}}{dt} + \int_{\nu=|t|}^{\nu=3.5} \nu \frac{d^2\sigma}{dt d\nu} d\nu$$

is equal, within the experimental accuracy of a few percent,  
 to the area under the curve of  $\nu d^2\sigma/dtd\nu$  obtained by extrapo-  
 lation of the high  $\nu$  data into the low  $\nu$  region.

# EXPERIMENTAL ARRANGEMENT

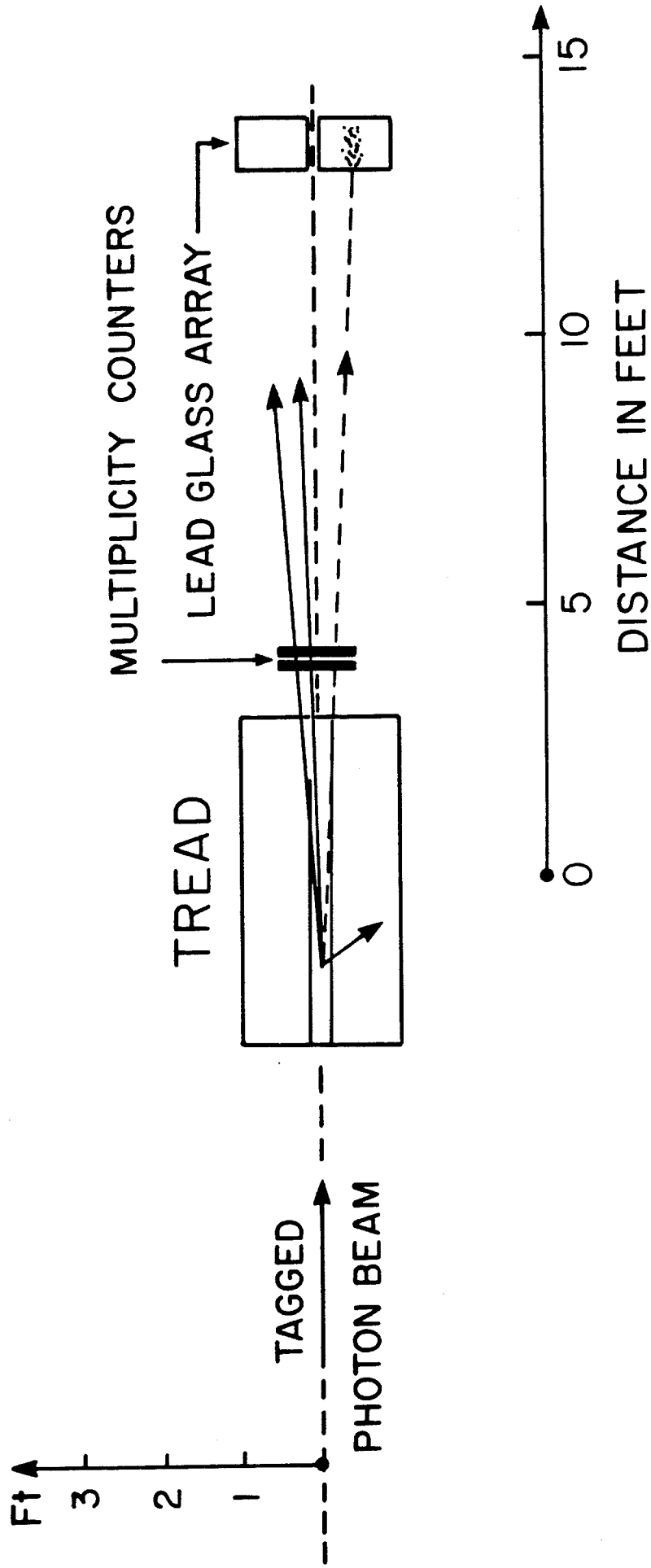


FIG. 3

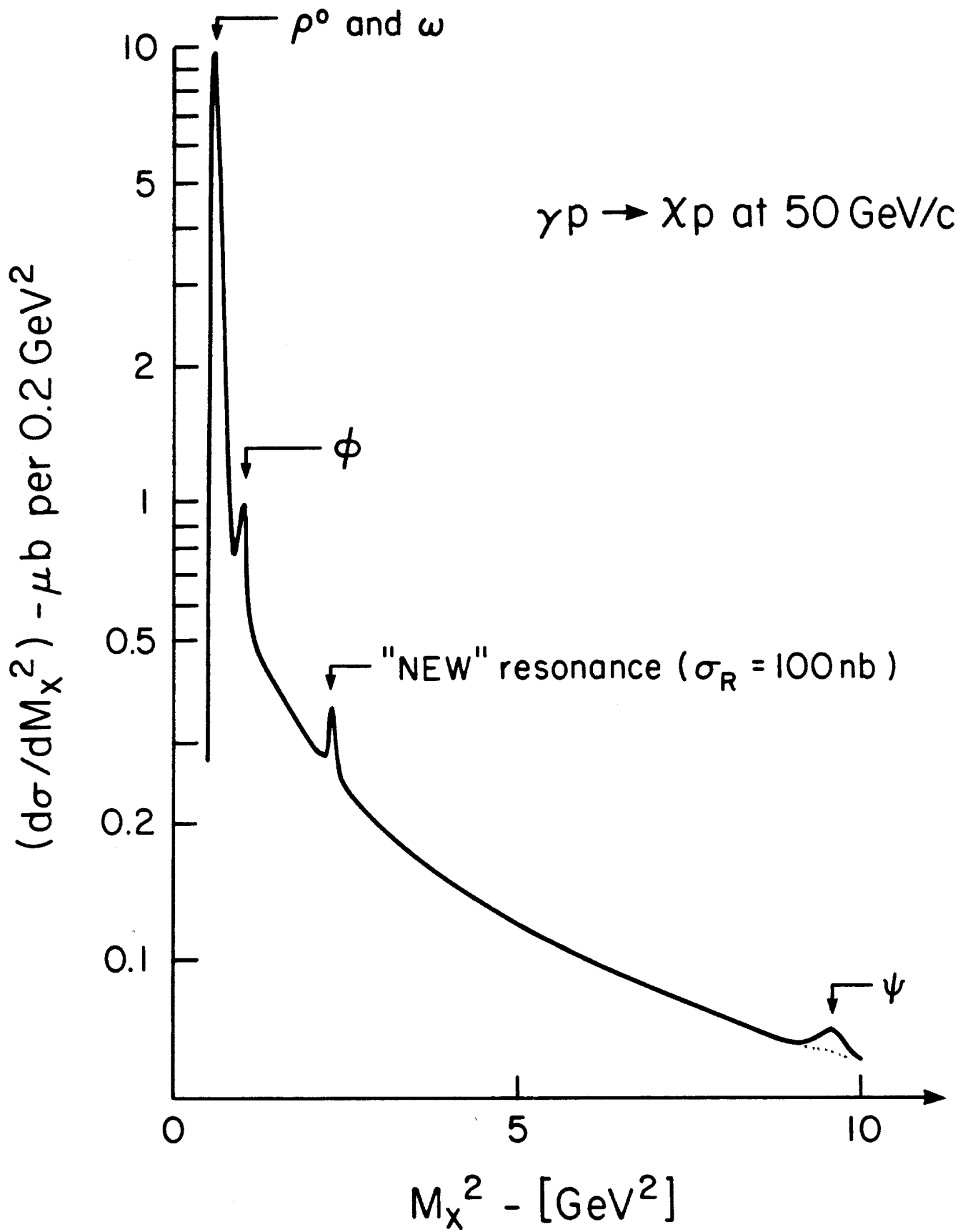


FIG. 4

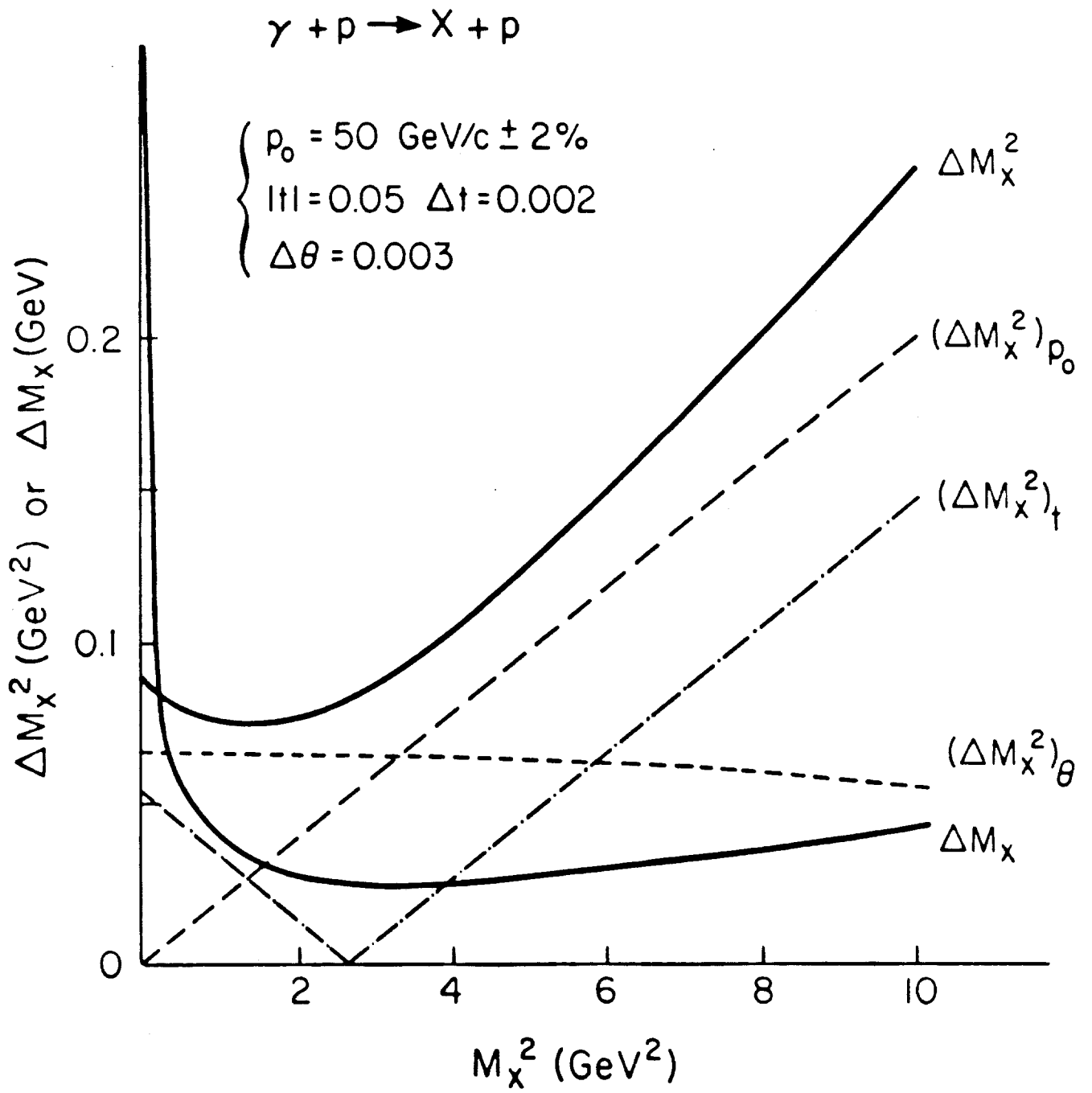


FIG. 5

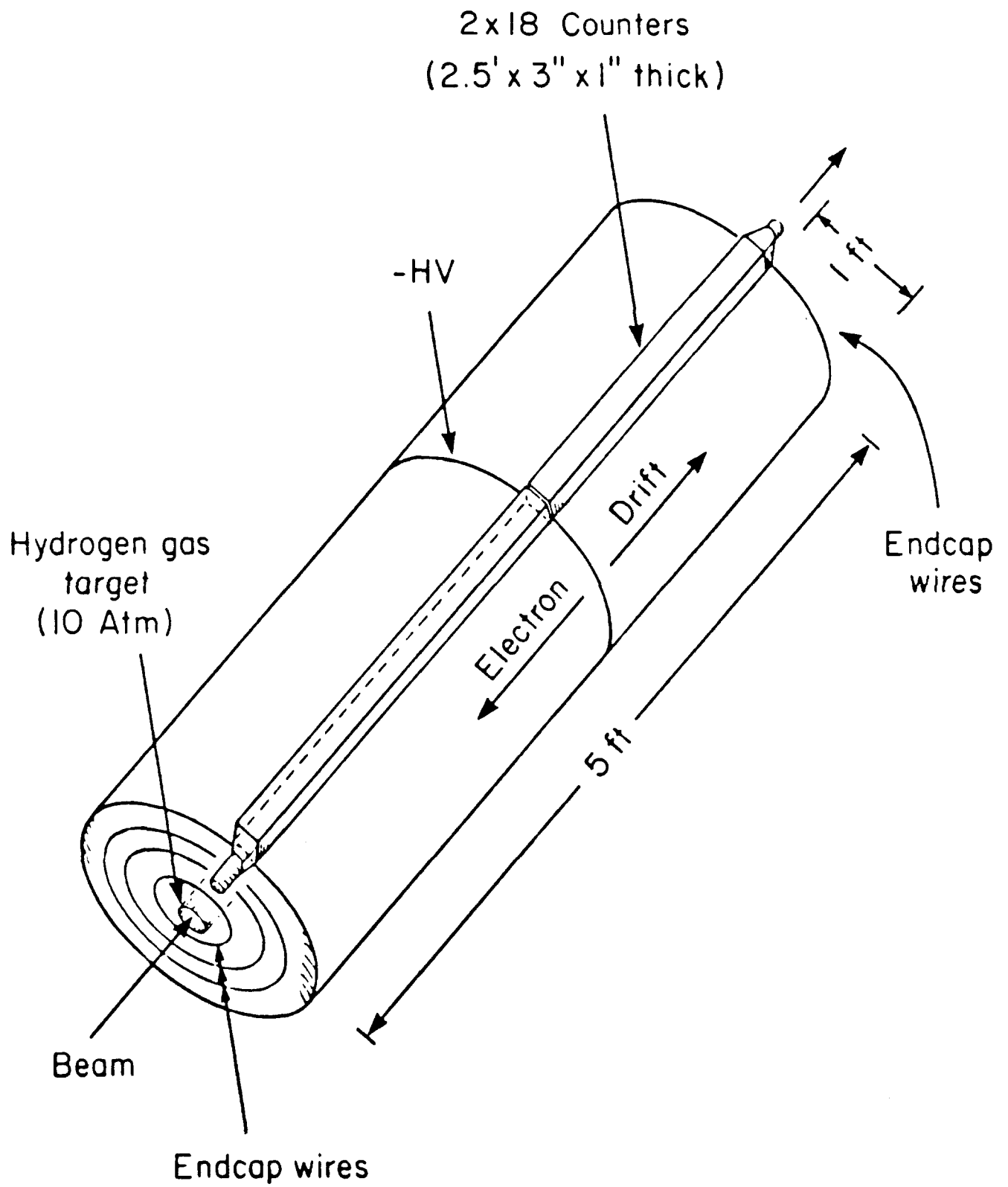


FIG. 6

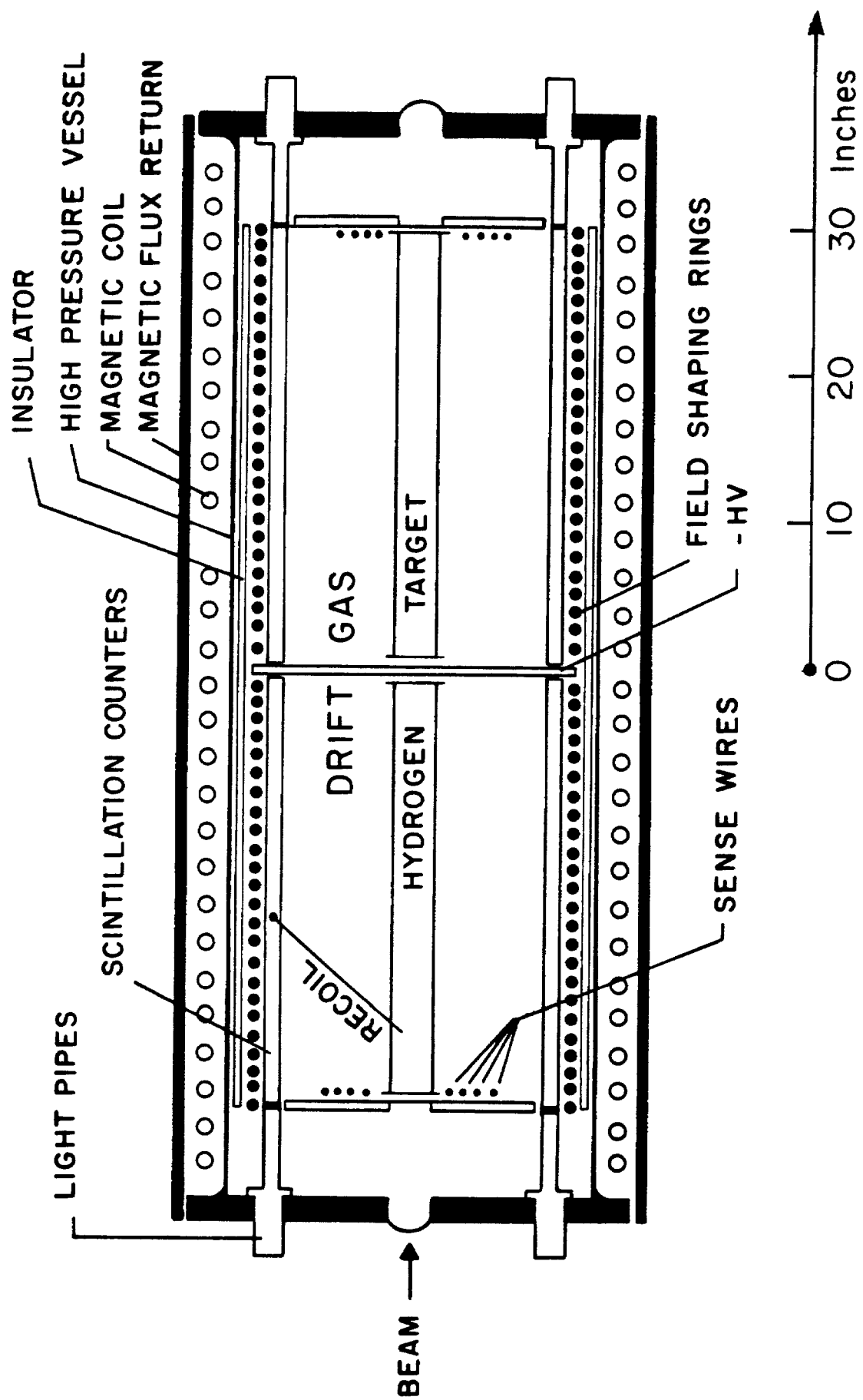
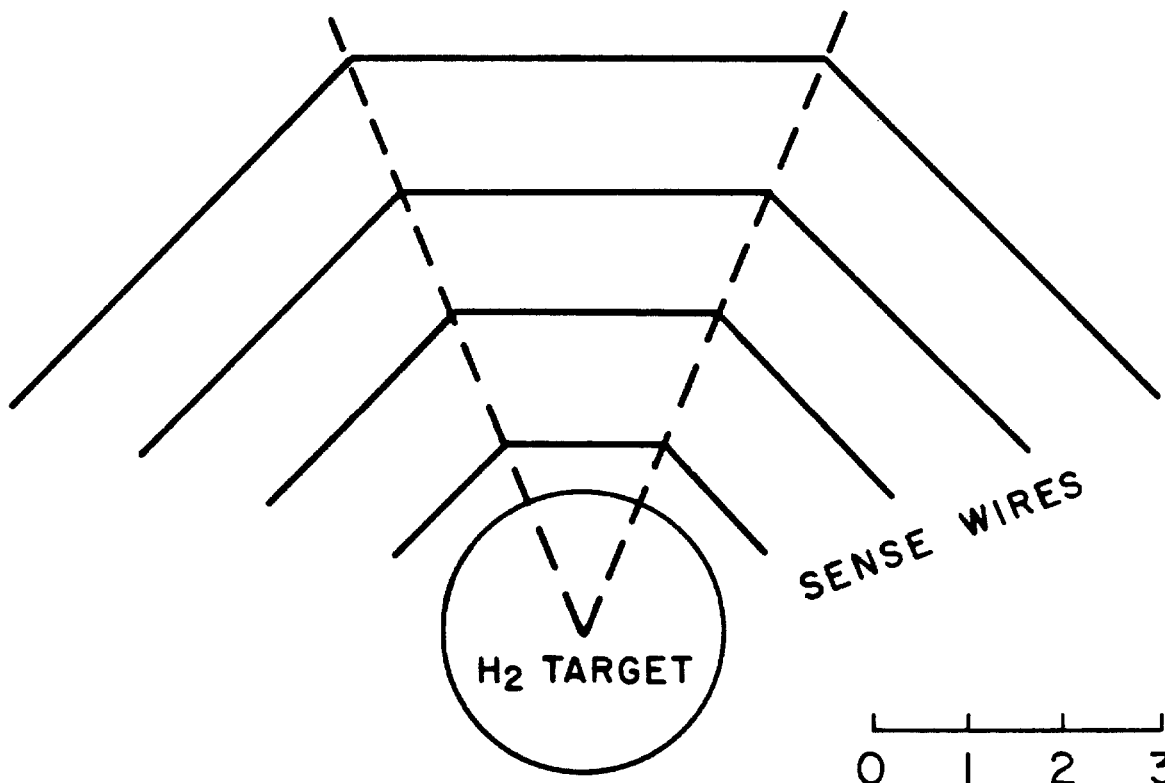
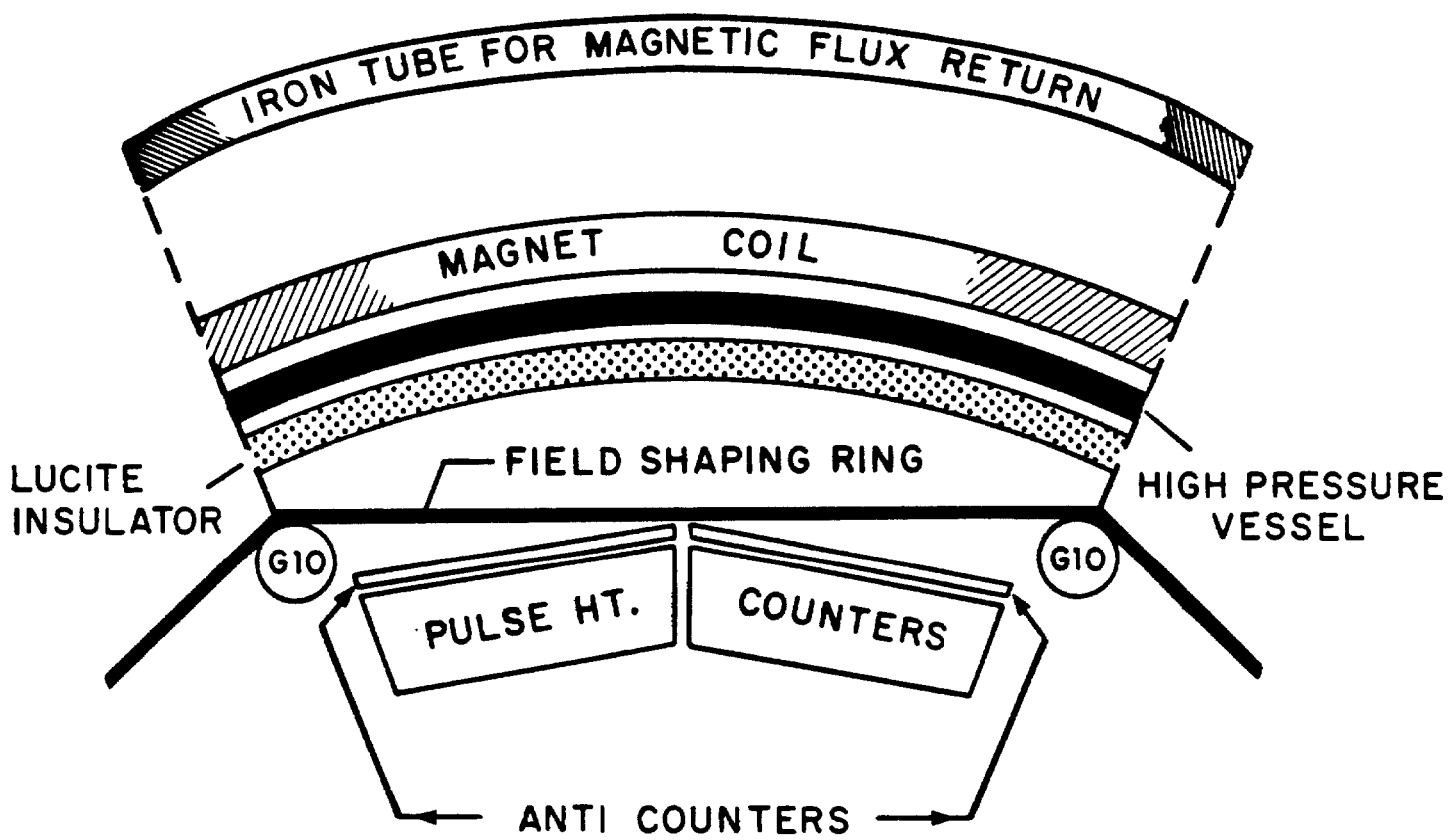


FIG. 7



0 1 2 3  
Scale (inches)

FIG. 8

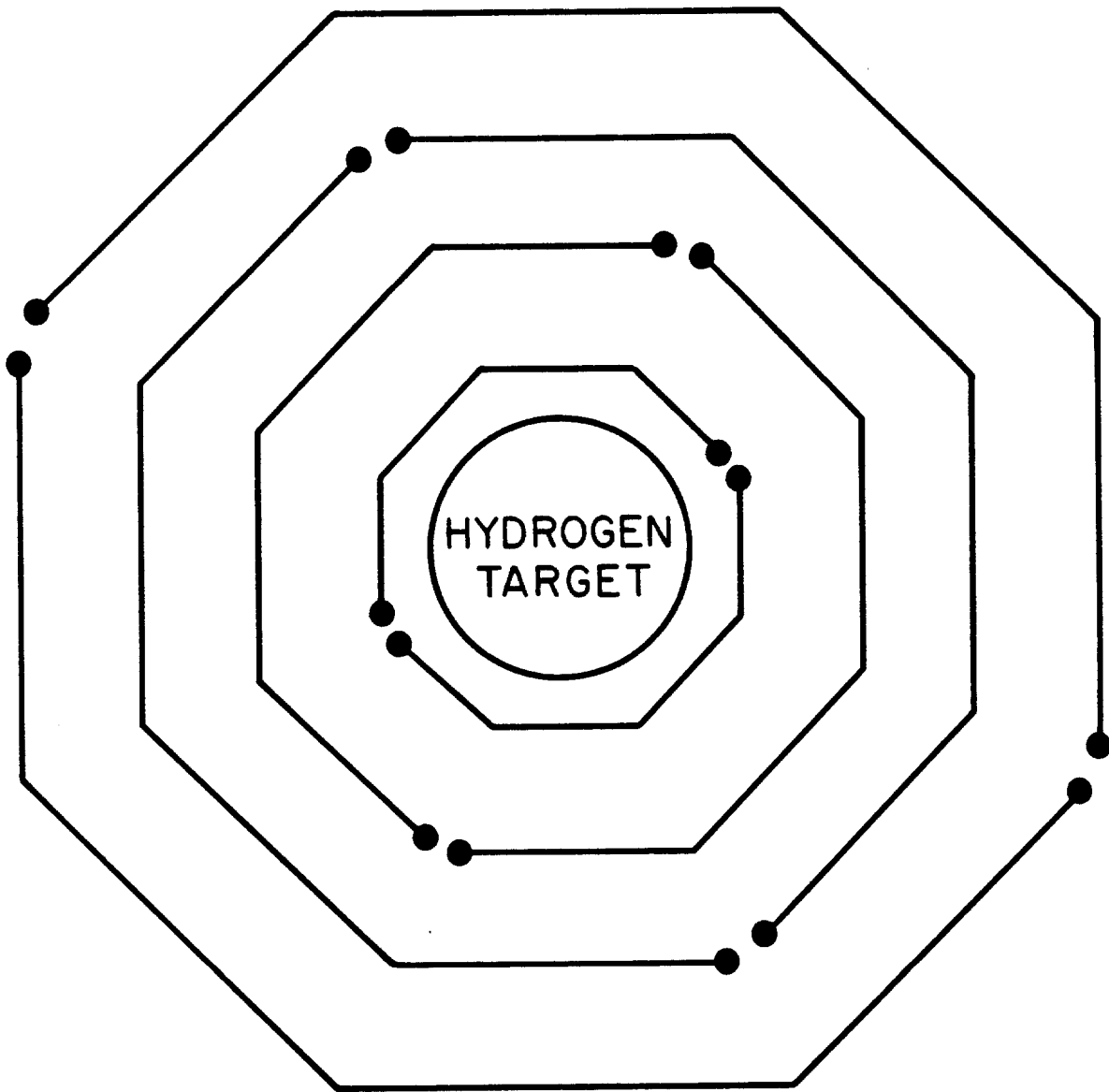


FIG. 9

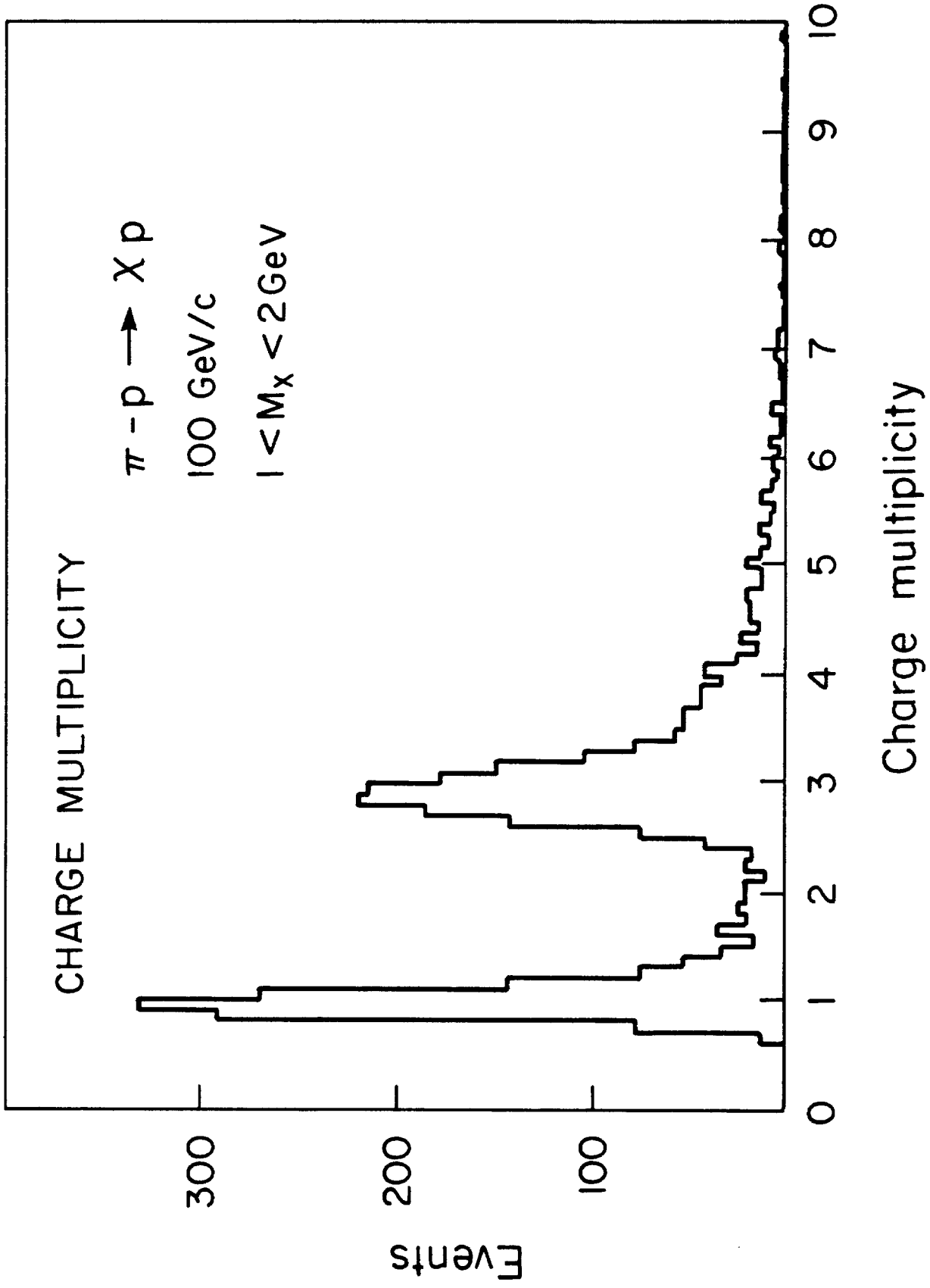


FIG. 10

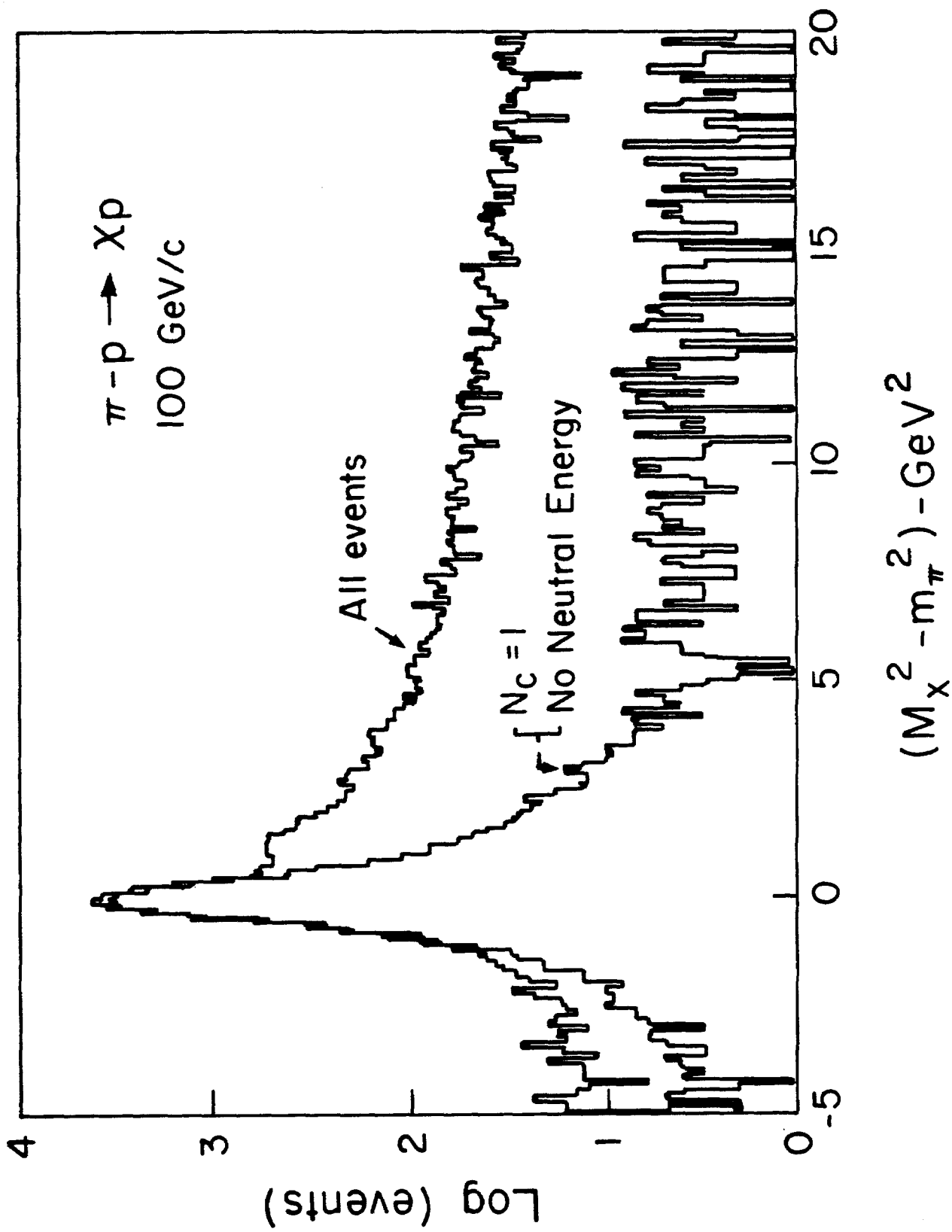


FIG. 11

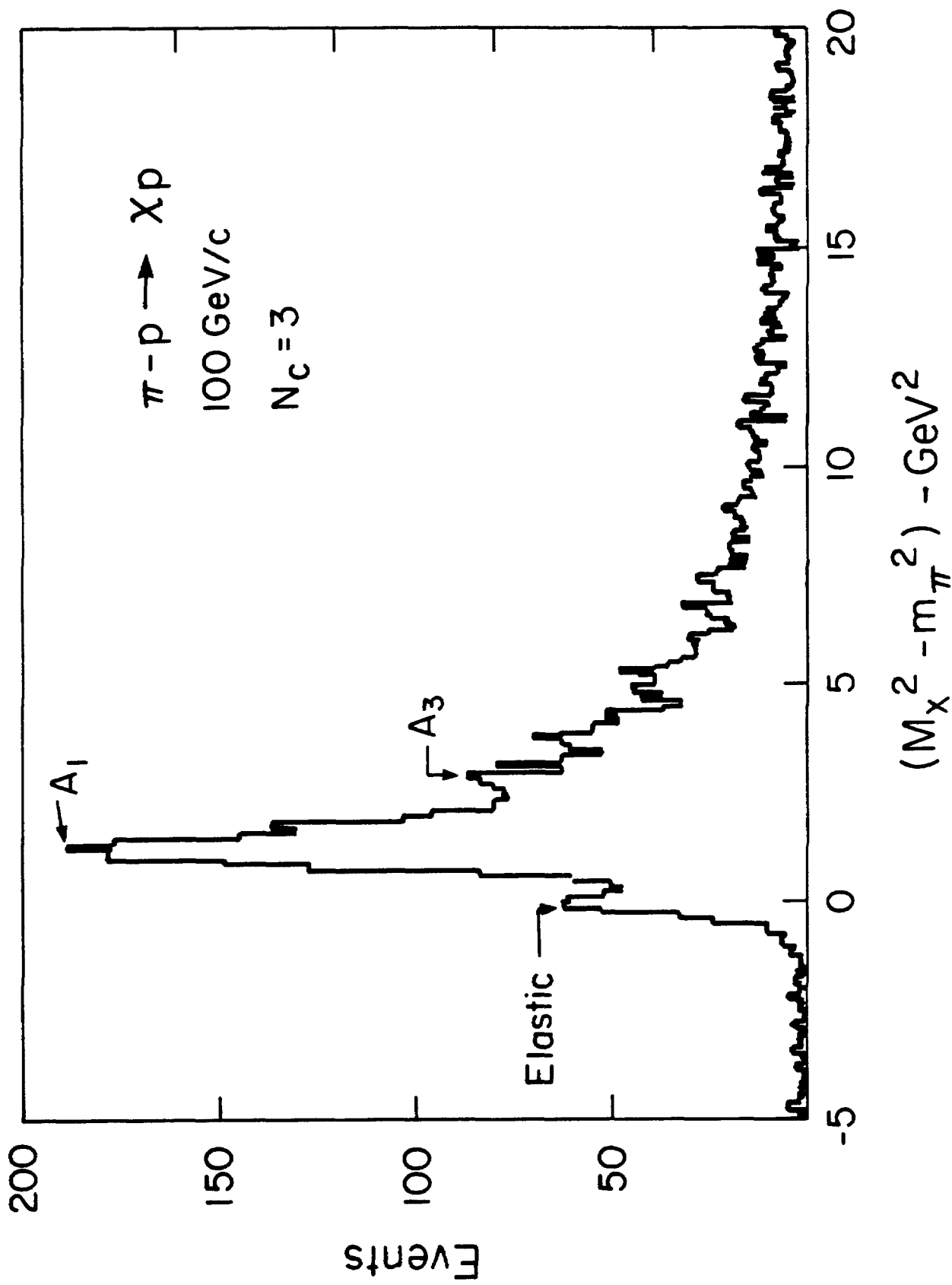


FIG.12

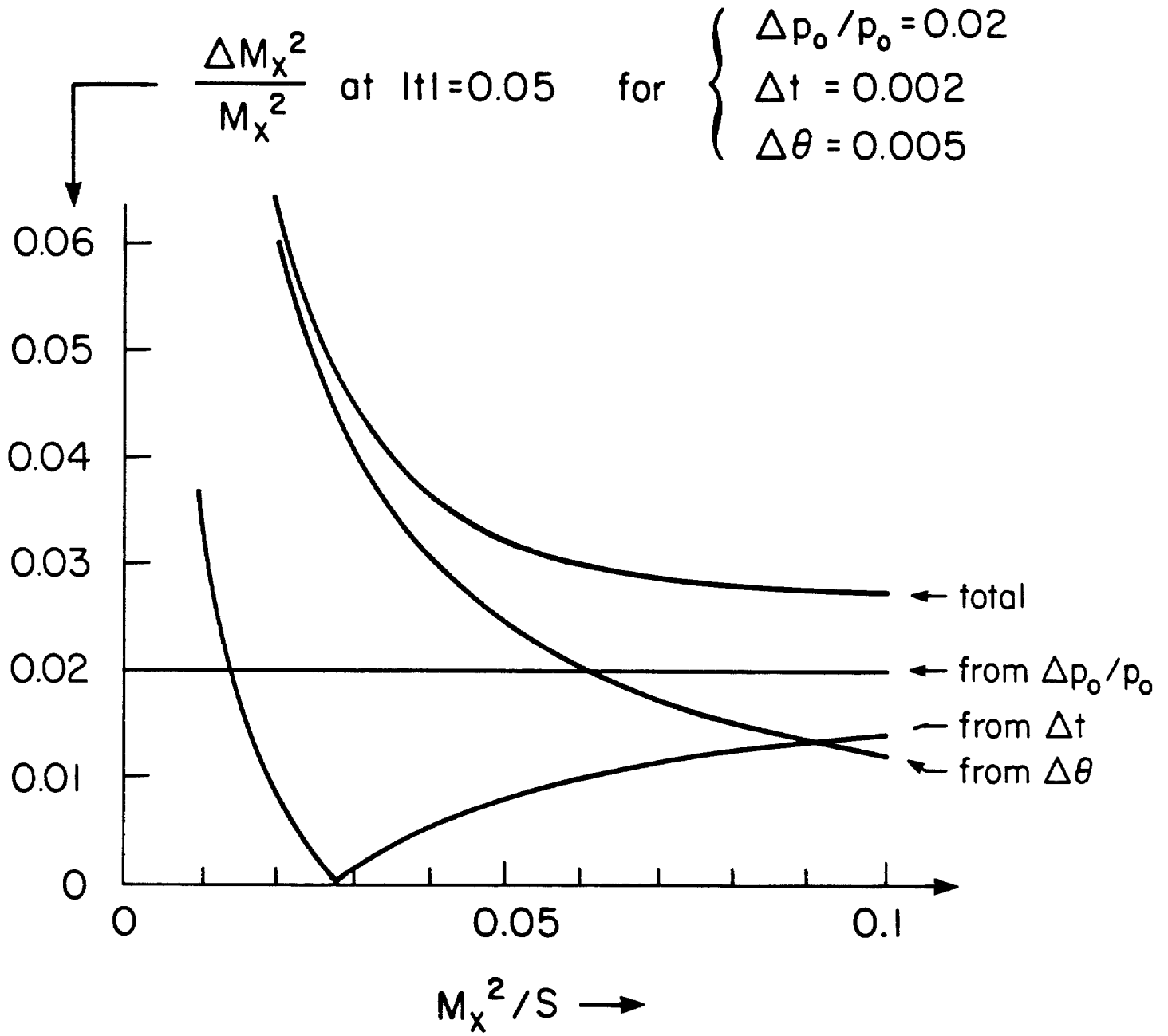


FIG. 13

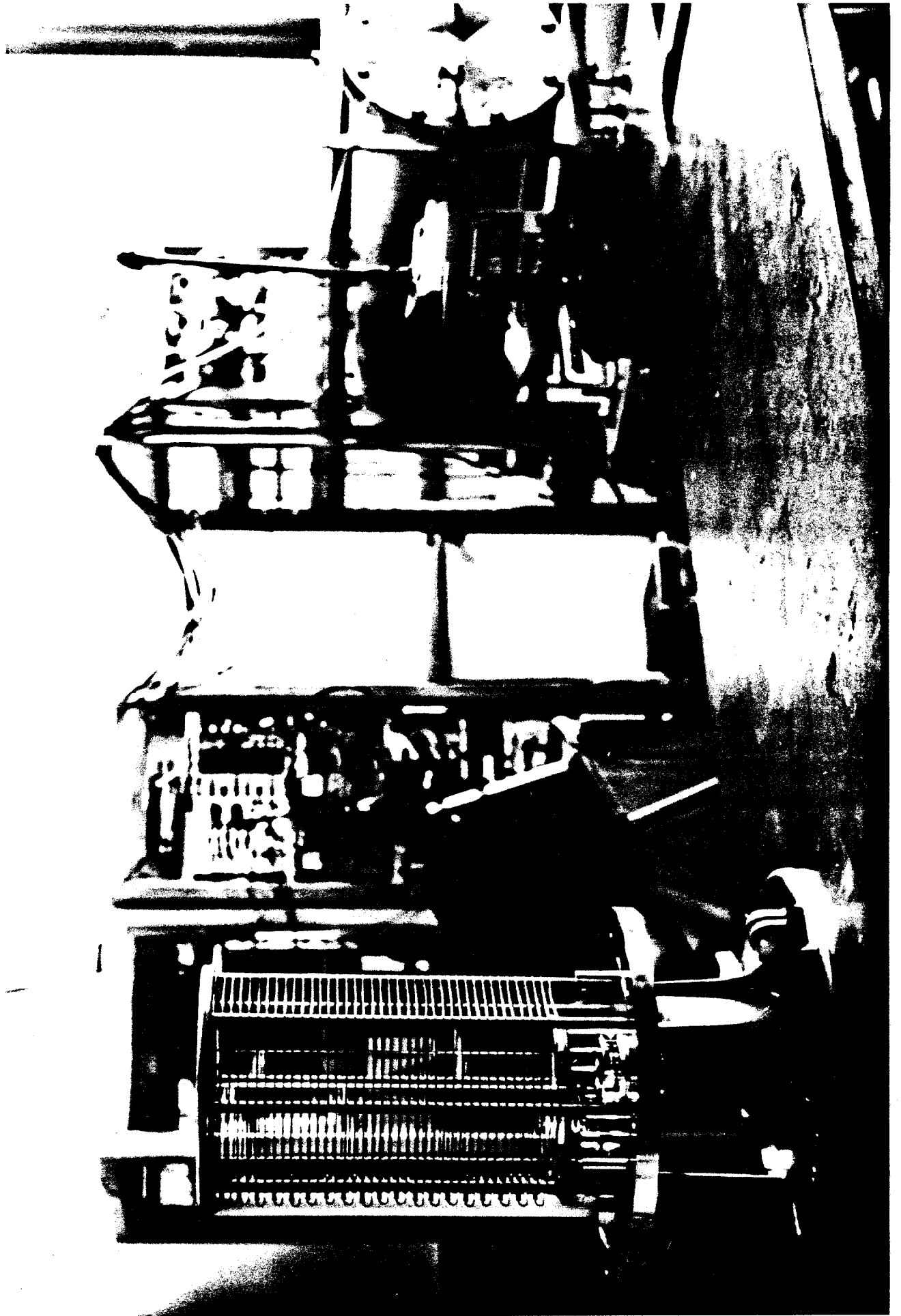


FIG. 14

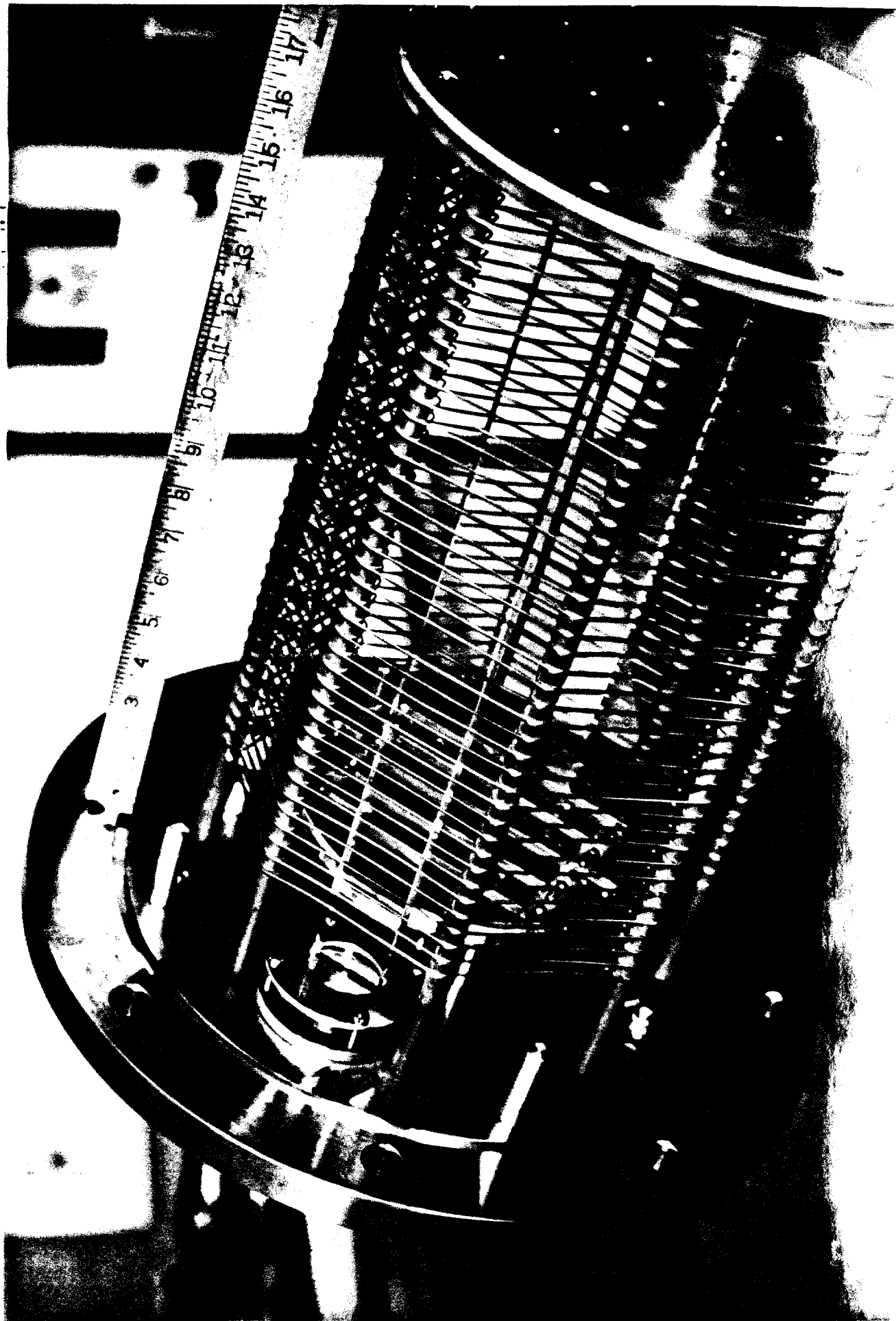


FIG. 15

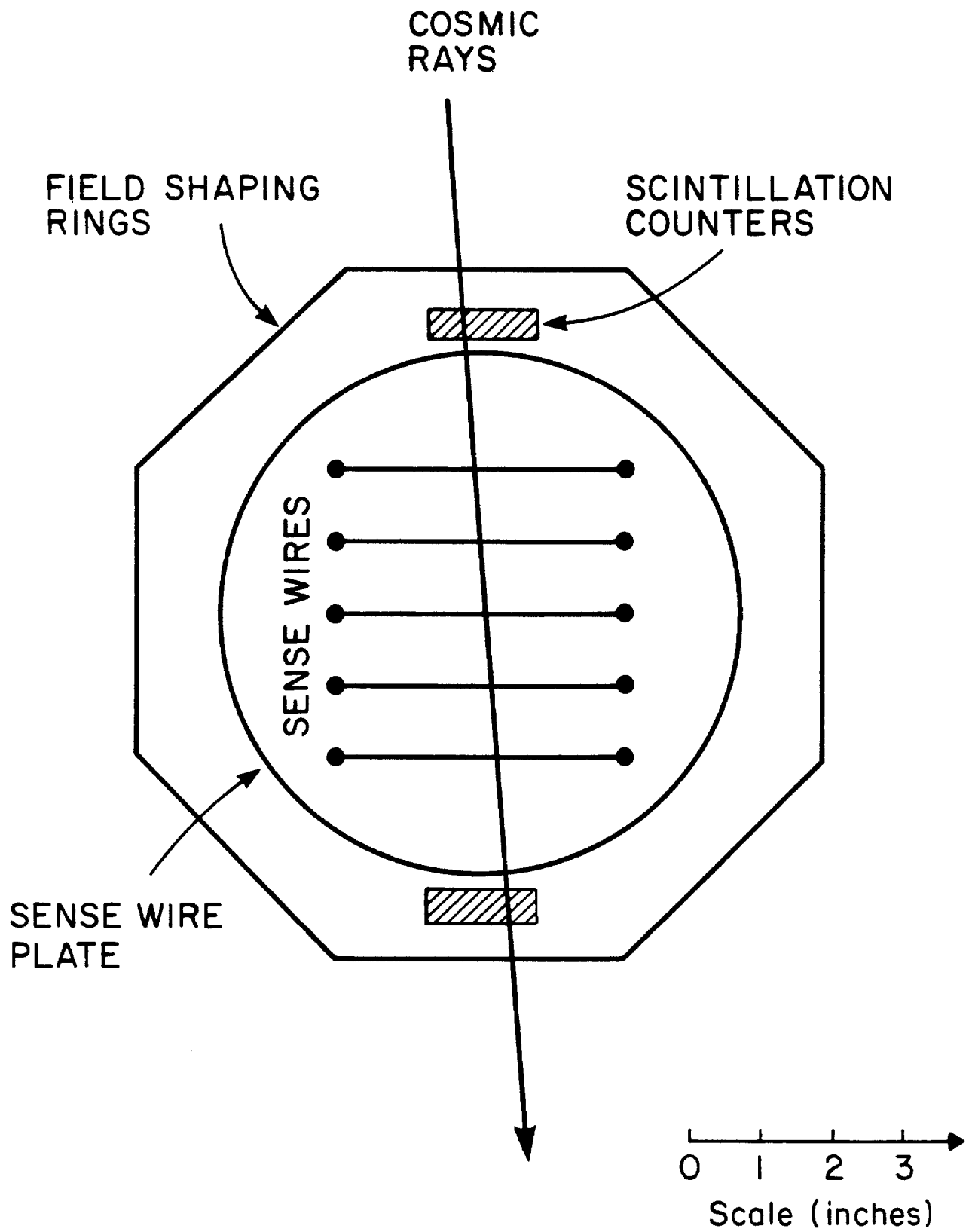
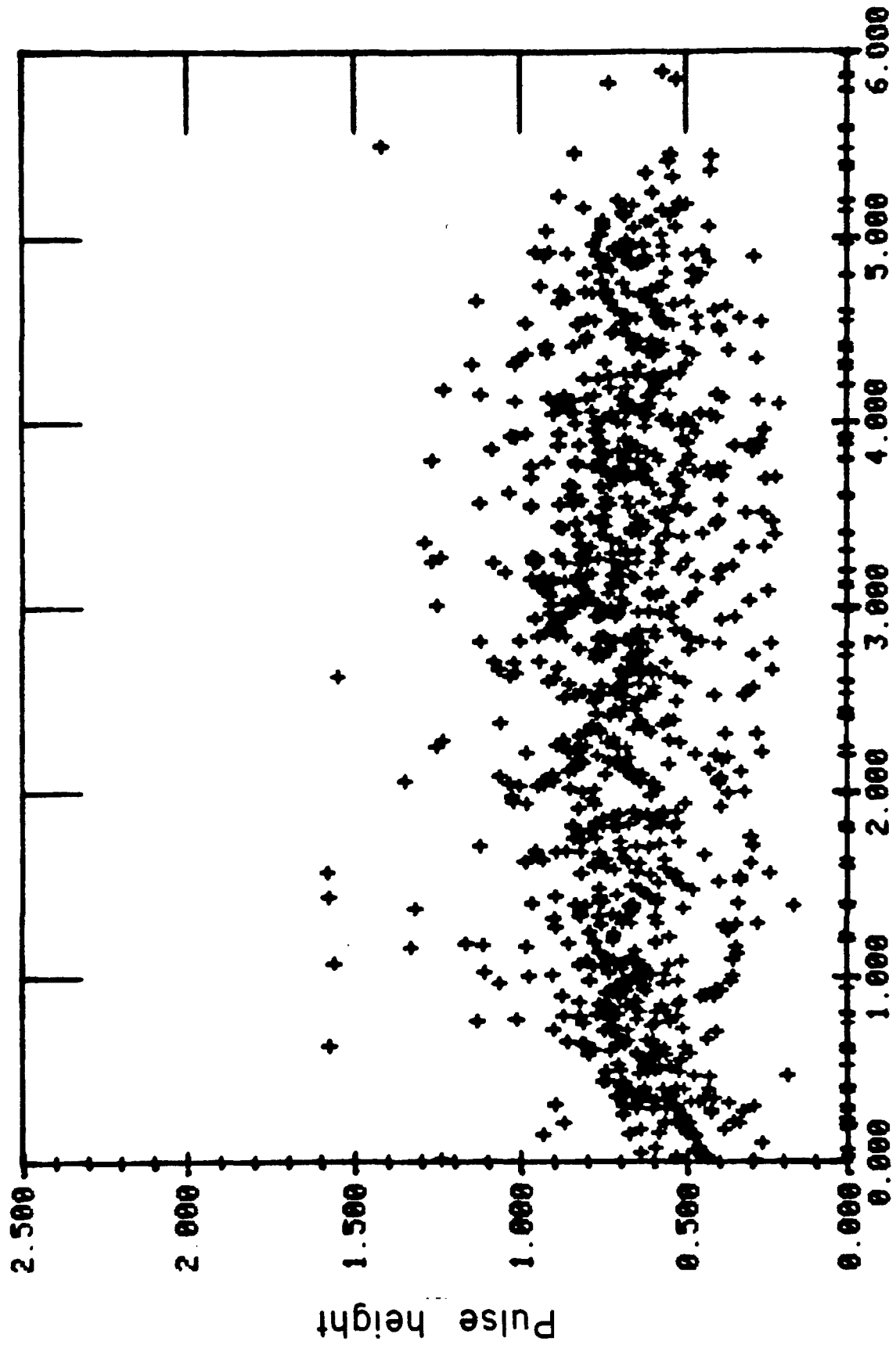


FIG. 16



Drift time - ( $\mu\text{sec} \times 10^{-1}$ )

FIG. 17

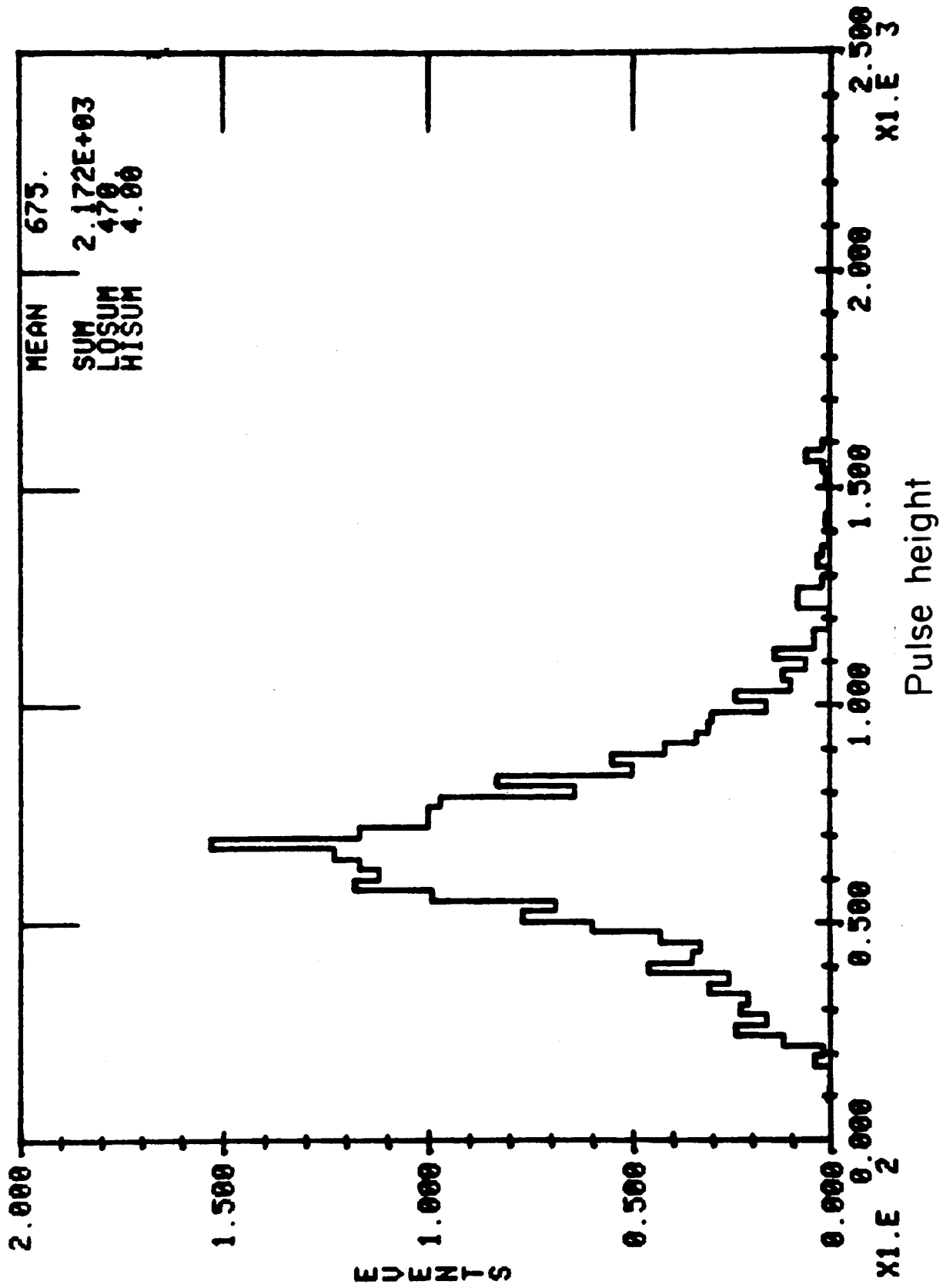
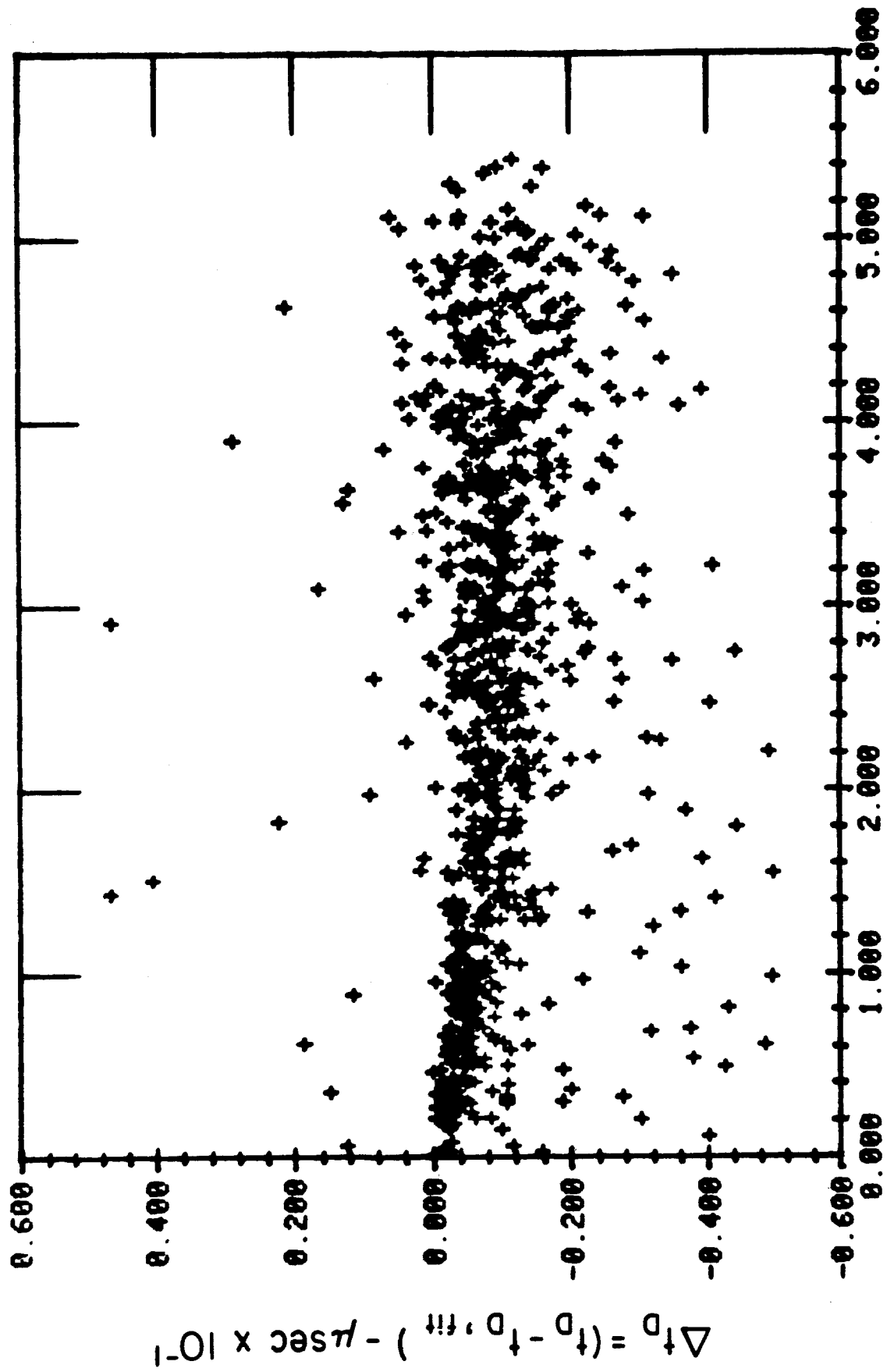


FIG 18



Drift time - ( $\mu\text{sec} \times 10^{-1}$ )

FIG.19